INDC (JPN)-181/U

NOT FOR PUBLICATION

PROGRESS REPORT

(January 1997 to December 1997 inclusive)

March 1998

Editor

J.Katakura

Japanese Nuclear Data Committee

Japan Atomic Energy Research Institute
Tokai Research Establishment
Tokai-mura, Naka-gun, Ibaraki-ken, Japan

Editor's Note

This is a collection of reports which have been submitted to the Japanese Nuclear Data Committee at the committee's request. The request was addressed to the following individuals who might represent or be touch with groups doing researches related to the nuclear data of interest to the development of the nuclear energy programs.

Although the editor tried not to miss any appropriate addressed, there may have been some oversight. Meanwhile, contribution of a report rested with discretion of its author. The coverage of this document, therefore, may not be uniform over the related field or research.

In this progress report, each individual report is generally reproduced as it was received by the JNDC secretariat, and editor also let pass some simple obvious errors in the manuscripts if any.

This edition covers a period of January 1, 1997 to December 31, 1997. The information herein contained is of a nature of "Private Communication." Data contained in this report should not be quoted without the author's permission.

Table of Contents

ELEMENT S	A	QUANTITY	ENERGY MIN	ENERGY MAX	LAB	TYPE	DOCUMENTATION REF	VOL	PAGE	DATE	COMMENTS
H	1	(N,GAMMA)	5.5+5		TIT	EXPT-PROG	INDC(JPN)-181U			MAR 98	NAGAI+.SIG=35.2+-2.4 MICRO BARNS
LI	6	N EMISSION	1.8+7		TOH	EXPT-PROG	INDC(JPN)-181U			MAR 98	IBARAKI+.DA/DE MEASUREMENT
LI	7	N EMISSION	1.8+7		TOH	EXPT-PROG	INDC(JPN)-181U			MAR 98	IBARAKI+.DA/DE MEASUREMENT
C		P EMISSION	6.4+7		TOH	EXPT-PROG	INDC(JPN)-181U			MAR 98	NAUCHI+.MEAS BY DEL E-E METHOD
C		D EMISSION	6.4+7		TOH	EXPT-PROG	INDC(JPN)-181U			MAR 98	NAUCHI+.MEAS BY DEL E-E METHOD
C	12	TOTAL	2.0+7	8.0+7	KYU	EVAL-PROG	INDC(JPN)-181U			MAR 98	HARADA+.FOR JENDL HIGH ENERGY FILE
C	12	ELASTIC	2.0+7	8.0+7	KYU	EVAL-PROG	INDC(JPN)-181U			MAR 98	HARADA+.FOR JENDL HIGH ENERGY FILE
C	12	DIFF ELASTIC	2.0+7	8.0+7	KYU	EVAL-PROG	INDC(JPN)-181U			MAR 98	HARADA+.FOR JENDL HIGH ENERGY FILE
C	12	TOT INELAST	2.0+7	8.0+7	KYU	EVAL-PROG	INDC(JPN)-181U			MAR 98	HARADA+.FOR JENDL HIGH ENERGY FILE
C	12	DIFF INELAST	2.0+7	8.0+7	KYU	EVAL-PROG	INDC(JPN)-181U			MAR 98	HARADA+.FOR JENDL HIGH ENERGY FILE
C	12	(N,GAMMA)	2.0+4	1.0+6	TIT	THEO-PROG	INDC(JPN)-181U			MAR 98	KITAZAWA+.DIRECT CAPTURE CALCULATION
C	12	(N,2N)	2.0+7	1.5+8	TOH	EXPT-PROG	INDC(JPN)-181U			MAR 98	KIM+.SIG IN FIG
C	12	N EMISSION	2.0+7	8.0+7	KYU	EVAL-PROG	INDC(JPN)-181U			MAR 98	HARADA+.FOR JENDL HIGH ENERGY FILE
C	12	P EMISSION	2.0+7	8.0+7	KYU	EVAL-PROG	INDC(JPN)-181U			MAR 98	HARADA+.FOR JENDL HIGH ENERGY FILE
C	12	D EMISSION	2.0+7	8.0+7	KYU	EVAL-PROG	INDC(JPN)-181U			MAR 98	HARADA+.FOR JENDL HIGH ENERGY FILE
C	12	T EMISSION	2.0+7	8.0+7	KYU	EVAL-PROG	INDC(JPN)-181U			MAR 98	HARADA+.FOR JENDL HIGH ENERGY FILE
C	12	(N,ALPHA)	1.4+7		TOH	EXPT-PROG	INDC(JPN)-181U			MAR 98	SANAMI+.GROUND STATE TRANSITION
C	12	A EMISSION	2.0+7	8.0+7	KYU	EVAL-PROG	INDC(JPN)-181U			MAR 98	HARADA+.FOR JENDL HIGH ENERGY FILE
C	12	NUCL PROD	2.0+7	8.0+7	KYU	EVAL-PROG	INDC(JPN)-181U			MAR 98	HARADA+.FOR JENDL HIGH ENERGY FILE
N	14	(N,P)	MAXW		TOH	EXPT-PROG	INDC(JPN)-181U			MAR 98	SANAMI+.KT=25.3 KEV.SIG=1.7+-.08 MB

ELEMENT S	A	QUANTITY	ENERGY MIN	ENERGY MAX	LAB	TYPE	DOCUMENTATION REF	VOL	PAGE	DATE	COMMENTS
O	16	(N,GAMMA)	2.0+4	3.0+5	TIT	THEO-PROG	INDC(JPN)-181U			MAR 98	KITAZAWA+.DIRECT CAPTURE CALCULATION
O	16	(N,ALPHA)	1.4+7		TOH	EXPT-PROG	INDC(JPN)-181U			MAR 98	SANAMI+.GRIDDED IONIZATION CHAMBER
F	19	SPECT (N,G)	2.7+4	9.7+4	TIT	EXPT-PROG	INDC(JPN)-181U			MAR 98	IGASHIRA+.ANTI-COMPTON NAI+GE
F	19	(N,P)	1.3+7	1.5+7	NAG	EXPT-PROG	INDC(JPN)-181U			MAR 98	KASUGAI+.ACT METH.REL AL-27(N,A) SIG
NA	23	SPECT (N,G)	3.5+4	5.3+4	TIT	EXPT-PROG	INDC(JPN)-181U			MAR 98	IGASHIRA+.ANTI-COMPTON NAI+GE
MG	26	(N,ALPHA)	1.3+7	1.5+7	NAG	EXPT-PROG	INDC(JPN)-181U			MAR 98	KASUGAI+.ACT METH.REL AL-27(N,A) SIG
AL		P EMISSION	6.4+7		TOH	EXPT-PROG	INDC(JPN)-181U			MAR 98	NAUCHI+.MEAS BY DEL E-E METHOD
AL		D EMISSION	6.4+7		TOH	EXPT-PROG	INDC(JPN)-181U			MAR 98	NAUCHI+.MEAS BY DEL E-E METHOD
AL	27	SPECT (N,G)	3.5+4		TIT	EXPT-PROG	INDC(JPN)-181U			MAR 98	IGASHIRA+.ANTI-COMPTON NAI+GE
AL	27	NUCL PROD	2.0+7	1.5+8	TOH	EXPT-PROG	INDC(JPN)-181U			MAR 98	KIM+.SIG IN FIG
SI	28	(N,P)	1.3+7	1.5+7	NAG	EXPT-PROG	INDC(JPN)-181U			MAR 98	KASUGAI+.ACT METH.REL AL-27(N,A) SIG
SI	29	(N,P)	1.3+7	1.5+7	NAG	EXPT-PROG	INDC(JPN)-181U			MAR 98	KASUGAI+.ACT METH.REL AL-27(N,A) SIG
P	31	(N,ALPHA)	1.3+7	1.5+7	NAG	EXPT-PROG	INDC(JPN)-181U			MAR 98	KASUGAI+.ACT METH.REL AL-27(N,A) SIG
CL	37	(N,P)	1.3+7	1.5+7	NAG	EXPT-PROG	INDC(JPN)-181U			MAR 98	KASUGAI+.ACT METH.REL AL-27(N,A) SIG
TI	50	(N,P)	1.3+7	1.5+7	NAG	EXPT-PROG	INDC(JPN)-181U			MAR 98	KASUGAI+.ACT METH.REL AL-27(N,A) SIG
V	51	SPECT (N,G)	5.5+5		TIT	EXPT-PROG	INDC(JPN)-181U			MAR 98	IGASHIRA+.LARGE ANTI-COMPTON NAI
V	51	P EMISSION	1.4+7		OSA	EXPT-PROG	INDC(JPN)-181U			MAR 98	TAKAHASHI+.DE IN FIG.SIG IN TABLE
V	51	A EMISSION	1.4+7		OSA	EXPT-PROG	INDC(JPN)-181U			MAR 98	TAKAHASHI+.SIG IN TABLE
CR	52	(N,P)	1.3+7	1.5+7	NAG	EXPT-PROG	INDC(JPN)-181U			MAR 98	KASUGAI+.ACT METH.REL AL-27(N,A) SIG
CR	53	(N,P)	1.3+7	1.5+7	NAG	EXPT-PROG	INDC(JPN)-181U			MAR 98	KASUGAI+.ACT METH.REL AL-27(N,A) SIG

ELEMENT S	A	QUANTITY	ENERGY MIN	ENERGY MAX	LAB	TYPE	DOCUMENTATION REF	VOL	PAGE	DATE	COMMENTS
CR	54	(N,P)	1.3+7	1.5+7	NAG	EXPT-PROG	INDC(JPN)-181U			MAR 98	KASUGAI+.ACT METH.REL AL-27(N,A) SIG
CR	54	(N,ALPHA)	1.3+7	1.5+7	NAG	EXPT-PROG	INDC(JPN)-181U			MAR 98	KASUGAI+.ACT METH.REL AL-27(N,A) SIG
MN	55	SPECT (N,G)	5.5+5		TIT	EXPT-PROG	INDC(JPN)-181U			MAR 98	IGASHIRA+.LARGE ANTI-COMPTON NAI
FE	CMP	A EMISSION	1.4+7		KYU	EXPT-PROG	INDC(JPN)-181U			MAR 98	TAKAO+.EFF SIG=52-59 MB +-8% ERROR
FE		A EMISSION	1.3+7	1.5+7	KYU	EXPT-PROG	INDC(JPN)-181U			MAR 98	TAKAO+.HELIUM ACCUMULATION METHOD
FE	56	TOTAL		2.0+7	KYU	THEO-PROG	INDC(JPN)-181U			MAR 98	KAWANO+.L-DEPENDENT OPTMDL POTENTIAL
CO	59	(N,XN) X>2	2.0+7	1.5+8	TOH	EXPT-PROG	INDC(JPN)-181U			MAR 98	KIM+.SIG IN FIG.X=3
NI	60	(N,P)	1.3+7	1.5+7	NAG	EXPT-PROG	INDC(JPN)-181U			MAR 98	KASUGAI+.ACT METH.REL AL-27(N,A) SIG
NI	62	(N,P)	1.3+7	1.5+7	NAG	EXPT-PROG	INDC(JPN)-181U			MAR 98	KASUGAI+.ACT METH.REL AL-27(N,A) SIG
NI	64	(N,ALPHA)	1.3+7	1.5+7	NAG	EXPT-PROG	INDC(JPN)-181U			MAR 98	KASUGAI+.ACT METH.REL AL-27(N,A) SIG
CU		NUCL PROD	2.0+7	1.5+8	TOH	EXPT-PROG	INDC(JPN)-181U			MAR 98	KIM+.SIG IN FIG
CU	63	(N,ALPHA)	1.3+7	1.5+7	NAG	EXPT-PROG	INDC(JPN)-181U			MAR 98	KASUGAI+.ACT METH.REL AL-27(N,A) SIG
ZN	66	(N,P)	1.3+7	1.5+7	NAG	EXPT-PROG	INDC(JPN)-181U			MAR 98	KASUGAI+.ACT METH.REL AL-27(N,A) SIG
ZN	68	(N,P)	1.3+7	1.5+7	NAG	EXPT-PROG	INDC(JPN)-181U			MAR 98	KASUGAI+.ACT METH.REL AL-27(N,A) SIG
GA	69	(N,ALPHA)	1.3+7	1.5+7	NAG	EXPT-PROG	INDC(JPN)-181U			MAR 98	KASUGAI+.ACT METH.REL AL-27(N,A) SIG
GA	71	(N,ALPHA)	1.3+7	1.5+7	NAG	EXPT-PROG	INDC(JPN)-181U			MAR 98	KASUGAI+.ACT METH.REL AL-27(N,A) SIG
RB	87	(N,ALPHA)	1.3+7	1.5+7	NAG	EXPT-PROG	INDC(JPN)-181U			MAR 98	KASUGAI+.ACT METH.REL AL-27(N,A) SIG
SR	86	(N,P)	1.3+7	1.5+7	NAG	EXPT-PROG	INDC(JPN)-181U			MAR 98	KASUGAI+.ACT METH.REL AL-27(N,A) SIG
SR	88	(N,P)	1.3+7	1.5+7	NAG	EXPT-PROG	INDC(JPN)-181U			MAR 98	KASUGAI+.ACT METH.REL AL-27(N,A) SIG
Y	89	(N,ALPHA)	1.3+7	1.5+7	NAG	EXPT-PROG	INDC(JPN)-181U			MAR 98	KASUGAI+.ACT METH.REL AL-27(N,A) SIG

ELEMENT S	A	QUANTITY	ENERGY MIN	ENERGY MAX	LAB	TYPE	DOCUMENTATION REF	VOL	PAGE	DATE	COMMENTS
ZR		P EMISSION	1.4+7		OSA	EXPT-PROG	INDC(JPN)-181U			MAR 98	TAKAHASHI+.DA/DE IN FIG
MO	97	(N,P)	1.3+7	1.5+7	NAG	EXPT-PROG	INDC(JPN)-181U			MAR 98	KASUGAI+.ACT METH.REL AL-27(N,A) SIG
RU	101	(N,P)	1.3+7	1.5+7	NAG	EXPT-PROG	INDC(JPN)-181U			MAR 98	KASUGAI+.ACT METH.REL AL-27(N,A) SIG
RU	102	(N,P)	1.3+7	1.5+7	NAG	EXPT-PROG	INDC(JPN)-181U			MAR 98	KASUGAI+.ACT METH.REL AL-27(N,A) SIG
RU	104	(N,P)	1.3+7	1.5+7	NAG	EXPT-PROG	INDC(JPN)-181U			MAR 98	KASUGAI+.ACT METH.REL AL-27(N,A) SIG
RU	104	(N,ALPHA)	1.3+7	1.5+7	NAG	EXPT-PROG	INDC(JPN)-181U			MAR 98	KASUGAI+.ACT METH.REL AL-27(N,A) SIG
PD	104	(N,P)	1.3+7	1.5+7	NAG	EXPT-PROG	INDC(JPN)-181U			MAR 98	KASUGAI+.ACT METH.REL AL-27(N,A) SIG
PD	105	(N,P)	1.3+7	1.5+7	NAG	EXPT-PROG	INDC(JPN)-181U			MAR 98	KASUGAI+.ACT METH.REL AL-27(N,A) SIG
PD	108	(N,P)	1.3+7	1.5+7	NAG	EXPT-PROG	INDC(JPN)-181U			MAR 98	KASUGAI+.ACT METH.REL AL-27(N,A) SIG
AG	107	(N,P)	1.3+7	1.5+7	NAG	EXPT-PROG	INDC(JPN)-181U			MAR 98	KASUGAI+.ACT METH.REL AL-27(N,A) SIG
CD	112	(N,ALPHA)	1.3+7	1.5+7	NAG	EXPT-PROG	INDC(JPN)-181U			MAR 98	KASUGAI+.ACT METH.REL AL-27(N,A) SIG
CD	116	(N,P)	1.3+7	1.5+7	NAG	EXPT-PROG	INDC(JPN)-181U			MAR 98	KASUGAI+.ACT METH.REL AL-27(N,A) SIG
SN	119	(N,P)	1.3+7	1.5+7	NAG	EXPT-PROG	INDC(JPN)-181U			MAR 98	KASUGAI+.ACT METH.REL AL-27(N,A) SIG
SN	120	(N,P)	1.3+7	1.5+7	NAG	EXPT-PROG	INDC(JPN)-181U			MAR 98	KASUGAI+.ACT METH.REL AL-27(N,A) SIG
I	127	(N,GAMMA)	2.5-2		PNC	EXPT-PROG	INDC(JPN)-181U			MAR 98	KATOH+.SIG GIVEN IN TABLE
I	127	RES INT CAP	NDG		PNC	EXPT-PROG	INDC(JPN)-181U			MAR 98	KATOH+.RI GIVEN IN TABLE
I	129	(N,2N)	1.3+7	1.5+7	OSA	EXPT-PROG	INDC(JPN)-181U			MAR 98	MURATA+.ACT METH.SIG GIVEN
CS	133	(N,GAMMA)	2.5-2		PNC	EXPT-PROG	INDC(JPN)-181U			MAR 98	NAKAMURA+.SIG GIVEN IN TABLE
CS	133	RES INT CAP	NDG		PNC	EXPT-PROG	INDC(JPN)-181U			MAR 98	NAKAMURA+.RI GIVEN IN TABLE
CS	135	(N,GAMMA)	2.5-2		PNC	EXPT-PROG	INDC(JPN)-181U			MAR 98	KATOH+.SIG=8.3+-0.3 BARNS

ELEMENT S	A	QUANTITY	ENERGY MIN	ENERGY MAX	LAB	TYPE	DOCUMENTATION REF	VOL	PAGE	DATE	COMMENTS
CS	135	RES INT CAP	NDG		PNC	EXPT-PROG	INDC(JPN)-181U			MAR 98	KATOH+.RI=38.1+-12.6 BARNS
CE	140	SPECT (N,G)	5.5+5		TIT	EXPT-PROG	INDC(JPN)-181U			MAR 98	IGASHIRA+.LARGE ANTI-COMPTON NAI
PR	141	SPECT (N,G)	5.5+5		TIT	EXPT-PROG	INDC(JPN)-181U			MAR 98	IGASHIRA+.LARGE ANTI-COMPTON NAI
SM	147	SPECT (N,G)	5.5+5		TIT	EXPT-PROG	INDC(JPN)-181U			MAR 98	IGASHIRA+.LARGE ANTI-COMPTON NAI
SM	150	SPECT (N,G)	5.5+5		TIT	EXPT-PROG	INDC(JPN)-181U			MAR 98	IGASHIRA+.LARGE ANTI-COMPTON NAI
SM	152	SPECT (N,G)	5.5+5		TIT	EXPT-PROG	INDC(JPN)-181U			MAR 98	IGASHIRA+.LARGE ANTI-COMPTON NAI
SM	154	SPECT (N,G)	5.5+5		TIT	EXPT-PROG	INDC(JPN)-181U			MAR 98	IGASHIRA+.LARGE ANTI-COMPTON NAI
EU	153	SPECT (N,G)	5.5+5		TIT	EXPT-PROG	INDC(JPN)-181U			MAR 98	IGASHIRA+.LARGE ANTI-COMPTON NAI
DY	162	SPECT (N,G)	5.5+5		TIT	EXPT-PROG	INDC(JPN)-181U			MAR 98	IGASHIRA+.LARGE ANTI-COMPTON NAI
HG	196	TOTAL	1.0-5	2.0+7	JAE	EVAL-PROG	INDC(JPN)-181U			MAR 98	SHIBATA+.EVALUATION FOR JENDL-3.3
HG	196	ELASTIC	1.0-5	2.0+7	JAE	EVAL-PROG	INDC(JPN)-181U			MAR 98	SHIBATA+.EVALUATION FOR JENDL-3.3
HG	196	DIFF ELASTIC	1.0-5	2.0+7	JAE	EVAL-PROG	INDC(JPN)-181U			MAR 98	SHIBATA+.EVALUATION FOR JENDL-3.3
HG	196	TOT INELAST	1.0-5	2.0+7	JAE	EVAL-PROG	INDC(JPN)-181U			MAR 98	SHIBATA+.EVALUATION FOR JENDL-3.3
HG	196	DIFF INELAST	1.0-5	2.0+7	JAE	EVAL-PROG	INDC(JPN)-181U			MAR 98	SHIBATA+.EVALUATION FOR JENDL-3.3
HG	196	(N,GAMMA)	1.0-5	2.0+7	JAE	EVAL-PROG	INDC(JPN)-181U			MAR 98	SHIBATA+.EVALUATION FOR JENDL-3.3
HG	196	SPECT (N,G)	1.0-5	2.0+7	JAE	EVAL-PROG	INDC(JPN)-181U			MAR 98	SHIBATA+.EVALUATION FOR JENDL-3.3
HG	196	INELA GAMMA	1.0-5	2.0+7	JAE	EVAL-PROG	INDC(JPN)-181U			MAR 98	SHIBATA+.EVALUATION FOR JENDL-3.3
HG	196	NONELA GAMMA	1.0-5	2.0+7	JAE	EVAL-PROG	INDC(JPN)-181U			MAR 98	SHIBATA+.EVALUATION FOR JENDL-3.3
HG	196	(N,2N)	1.0-5	2.0+7	JAE	EVAL-PROG	INDC(JPN)-181U			MAR 98	SHIBATA+.EVALUATION FOR JENDL-3.3
HG	196	(N,XN) X>2	1.0-5	2.0+7	JAE	EVAL-PROG	INDC(JPN)-181U			MAR 98	SHIBATA+.EVALUATION FOR JENDL-3.3

ELEMENT S	A	QUANTITY	ENERGY MIN	ENERGY MAX	LAB	TYPE	DOCUMENTATION REF	VOL	PAGE	DATE	COMMENTS
HG	196	(N,P)	1.0-5	2.0+7	JAE	EVAL-PROG	INDC(JPN)-181U			MAR 98	SHIBATA+.EVALUATION FOR JENDL-3.3
HG	196	(N,NP)	1.0-5	2.0+7	JAE	EVAL-PROG	INDC(JPN)-181U			MAR 98	SHIBATA+.EVALUATION FOR JENDL-3.3
HG	196	(N,ALPHA)	1.0-5	2.0+7	JAE	EVAL-PROG	INDC(JPN)-181U			MAR 98	SHIBATA+.EVALUATION FOR JENDL-3.3
HG	196	(N,NA)	1.0-5	2.0+7	JAE	EVAL-PROG	INDC(JPN)-181U			MAR 98	SHIBATA+.EVALUATION FOR JENDL-3.3
HG	196	RESON PARAMS	1.0-5	2.0+7	JAE	EVAL-PROG	INDC(JPN)-181U			MAR 98	SHIBATA+.EVALUATION FOR JENDL-3.3
HG	198	TOTAL	1.0-5	2.0+7	JAE	EVAL-PROG	INDC(JPN)-181U			MAR 98	SHIBATA+.EVALUATION FOR JENDL-3.3
HG	198	ELASTIC	1.0-5	2.0+7	JAE	EVAL-PROG	INDC(JPN)-181U			MAR 98	SHIBATA+.EVALUATION FOR JENDL-3.3
HG	198	DIFF ELASTIC	1.0-5	2.0+7	JAE	EVAL-PROG	INDC(JPN)-181U			MAR 98	SHIBATA+.EVALUATION FOR JENDL-3.3
HG	198	TOT INELAST	1.0-5	2.0+7	JAE	EVAL-PROG	INDC(JPN)-181U			MAR 98	SHIBATA+.EVALUATION FOR JENDL-3.3
HG	198	DIFF INELAST	1.0-5	2.0+7	JAE	EVAL-PROG	INDC(JPN)-181U			MAR 98	SHIBATA+.EVALUATION FOR JENDL-3.3
HG	198	(N,GAMMA)	1.0-5	2.0+7	JAE	EVAL-PROG	INDC(JPN)-181U			MAR 98	SHIBATA+.EVALUATION FOR JENDL-3.3
HG	198	SPECT (N,G)	1.0-5	2.0+7	JAE	EVAL-PROG	INDC(JPN)-181U			MAR 98	SHIBATA+.EVALUATION FOR JENDL-3.3
HG	198	INELA GAMMA	1.0-5	2.0+7	JAE	EVAL-PROG	INDC(JPN)-181U			MAR 98	SHIBATA+.EVALUATION FOR JENDL-3.3
HG	198	NONELA GAMMA	1.0-5	2.0+7	JAE	EVAL-PROG	INDC(JPN)-181U			MAR 98	SHIBATA+.EVALUATION FOR JENDL-3.3
HG	198	(N,2N)	1.0-5	2.0+7	JAE	EVAL-PROG	INDC(JPN)-181U			MAR 98	SHIBATA+.EVALUATION FOR JENDL-3.3
HG	198	(N,XN) X>2	1.0-5	2.0+7	JAE	EVAL-PROG	INDC(JPN)-181U			MAR 98	SHIBATA+.EVALUATION FOR JENDL-3.3
HG	198	(N,P)	1.0-5	2.0+7	JAE	EVAL-PROG	INDC(JPN)-181U			MAR 98	SHIBATA+.EVALUATION FOR JENDL-3.3
HG	198	(N,NP)	1.0-5	2.0+7	JAE	EVAL-PROG	INDC(JPN)-181U			MAR 98	SHIBATA+.EVALUATION FOR JENDL-3.3
HG	198	(N,ALPHA)	1.0-5	2.0+7	JAE	EVAL-PROG	INDC(JPN)-181U			MAR 98	SHIBATA+.EVALUATION FOR JENDL-3.3
HG	198	(N,NA)	1.0-5	2.0+7	JAE	EVAL-PROG	INDC(JPN)-181U			MAR 98	SHIBATA+.EVALUATION FOR JENDL-3.3

ELEMENT S	A	QUANTITY	ENERGY MIN	ENERGY MAX	LAB	TYPE	DOCUMENTATION REF	VOL	PAGE	DATE	COMMENTS
HG	198	RESON PARAMS	1.0-5	2.0+7	JAE	EVAL-PROG	INDC(JPN)-181U			MAR 98	SHIBATA+.EVALUATION FOR JENDL-3.3
HG	199	TOTAL	1.0-5	2.0+7	JAE	EVAL-PROG	INDC(JPN)-181U			MAR 98	SHIBATA+.EVALUATION FOR JENDL-3.3
HG	199	ELASTIC	1.0-5	2.0+7	JAE	EVAL-PROG	INDC(JPN)-181U			MAR 98	SHIBATA+.EVALUATION FOR JENDL-3.3
HG	199	DIFF ELASTIC	1.0-5	2.0+7	JAE	EVAL-PROG	INDC(JPN)-181U			MAR 98	SHIBATA+.EVALUATION FOR JENDL-3.3
HG	199	TOT INELAST	1.0-5	2.0+7	JAE	EVAL-PROG	INDC(JPN)-181U			MAR 98	SHIBATA+.EVALUATION FOR JENDL-3.3
HG	199	DIFF INELAST	1.0-5	2.0+7	JAE	EVAL-PROG	INDC(JPN)-181U			MAR 98	SHIBATA+.EVALUATION FOR JENDL-3.3
HG	199	(N,GAMMA)	1.0-5	2.0+7	JAE	EVAL-PROG	INDC(JPN)-181U			MAR 98	SHIBATA+.EVALUATION FOR JENDL-3.3
HG	199	SPECT (N,G)	1.0-5	2.0+7	JAE	EVAL-PROG	INDC(JPN)-181U			MAR 98	SHIBATA+.EVALUATION FOR JENDL-3.3
HG	199	INELA GAMMA	1.0-5	2.0+7	JAE	EVAL-PROG	INDC(JPN)-181U			MAR 98	SHIBATA+.EVALUATION FOR JENDL-3.3
HG	199	NONELA GAMMA	1.0-5	2.0+7	JAE	EVAL-PROG	INDC(JPN)-181U			MAR 98	SHIBATA+.EVALUATION FOR JENDL-3.3
HG	199	(N,2N)	1.0-5	2.0+7	JAE	EVAL-PROG	INDC(JPN)-181U			MAR 98	SHIBATA+.EVALUATION FOR JENDL-3.3
HG	199	(N,XN) X>2	1.0-5	2.0+7	JAE	EVAL-PROG	INDC(JPN)-181U			MAR 98	SHIBATA+.EVALUATION FOR JENDL-3.3
HG	199	(N,P)	1.0-5	2.0+7	JAE	EVAL-PROG	INDC(JPN)-181U			MAR 98	SHIBATA+.EVALUATION FOR JENDL-3.3
HG	199	(N,NP)	1.0-5	2.0+7	JAE	EVAL-PROG	INDC(JPN)-181U			MAR 98	SHIBATA+.EVALUATION FOR JENDL-3.3
HG	199	(N,ALPHA)	1.0-5	2.0+7	JAE	EVAL-PROG	INDC(JPN)-181U			MAR 98	SHIBATA+.EVALUATION FOR JENDL-3.3
HG	199	(N,NA)	1.0-5	2.0+7	JAE	EVAL-PROG	INDC(JPN)-181U			MAR 98	SHIBATA+.EVALUATION FOR JENDL-3.3
HG	199	RESON PARAMS	1.0-5	2.0+7	JAE	EVAL-PROG	INDC(JPN)-181U			MAR 98	SHIBATA+.EVALUATION FOR JENDL-3.3
HG	200	TOTAL	1.0-5	2.0+7	JAE	EVAL-PROG	INDC(JPN)-181U			MAR 98	SHIBATA+.EVALUATION FOR JENDL-3.3
HG	200	ELASTIC	1.0-5	2.0+7	JAE	EVAL-PROG	INDC(JPN)-181U			MAR 98	SHIBATA+.EVALUATION FOR JENDL-3.3
HG	200	DIFF ELASTIC	1.0-5	2.0+7	JAE	EVAL-PROG	INDC(JPN)-181U			MAR 98	SHIBATA+.EVALUATION FOR JENDL-3.3

ELEMENT S	A	QUANTITY	ENERGY MIN	ENERGY MAX	LAB	TYPE	DOCUMENTATION REF	VOL	PAGE	DATE	COMMENTS
HG	200	TOT INELAST	1.0-5	2.0+7	JAE	EVAL-PROG	INDC(JPN)-181U			MAR 98	SHIBATA+.EVALUATION FOR JENDL-3.3
HG	200	DIFF INELAST	1.0-5	2.0+7	JAE	EVAL-PROG	INDC(JPN)-181U			MAR 98	SHIBATA+.EVALUATION FOR JENDL-3.3
HG	200	(N,GAMMA)	1.0-5	2.0+7	JAE	EVAL-PROG	INDC(JPN)-181U			MAR 98	SHIBATA+.EVALUATION FOR JENDL-3.3
HG	200	SPECT (N,G)	1.0-5	2.0+7	JAE	EVAL-PROG	INDC(JPN)-181U			MAR 98	SHIBATA+.EVALUATION FOR JENDL-3.3
HG	200	INELA GAMMA	1.0-5	2.0+7	JAE	EVAL-PROG	INDC(JPN)-181U			MAR 98	SHIBATA+.EVALUATION FOR JENDL-3.3
HG	200	NONELA GAMMA	1.0-5	2.0+7	JAE	EVAL-PROG	INDC(JPN)-181U			MAR 98	SHIBATA+.EVALUATION FOR JENDL-3.3
HG	200	(N,2N)	1.0-5	2.0+7	JAE	EVAL-PROG	INDC(JPN)-181U			MAR 98	SHIBATA+.EVALUATION FOR JENDL-3.3
HG	200	(N,XN) X>2	1.0-5	2.0+7	JAE	EVAL-PROG	INDC(JPN)-181U			MAR 98	SHIBATA+.EVALUATION FOR JENDL-3.3
HG	200	(N,P)	1.0-5	2.0+7	JAE	EVAL-PROG	INDC(JPN)-181U			MAR 98	SHIBATA+.EVALUATION FOR JENDL-3.3
HG	200	(N,NP)	1.0-5	2.0+7	JAE	EVAL-PROG	INDC(JPN)-181U			MAR 98	SHIBATA+.EVALUATION FOR JENDL-3.3
HG	200	(N,ALPHA)	1.0-5	2.0+7	JAE	EVAL-PROG	INDC(JPN)-181U			MAR 98	SHIBATA+.EVALUATION FOR JENDL-3.3
HG	200	(N,NA)	1.0-5	2.0+7	JAE	EVAL-PROG	INDC(JPN)-181U			MAR 98	SHIBATA+.EVALUATION FOR JENDL-3.3
HG	200	RESON PARAMS	1.0-5	2.0+7	JAE	EVAL-PROG	INDC(JPN)-181U			MAR 98	SHIBATA+.EVALUATION FOR JENDL-3.3
HG	201	ELASTIC	1.0-5	2.0+7	JAE	EVAL-PROG	INDC(JPN)-181U			MAR 98	SHIBATA+.EVALUATION FOR JENDL-3.3
HG	201	DIFF ELASTIC	1.0-5	2.0+7	JAE	EVAL-PROG	INDC(JPN)-181U			MAR 98	SHIBATA+.EVALUATION FOR JENDL-3.3
HG	201	TOT INELAST	1.0-5	2.0+7	JAE	EVAL-PROG	INDC(JPN)-181U			MAR 98	SHIBATA+.EVALUATION FOR JENDL-3.3
HG	201	DIFF INELAST	1.0-5	2.0+7	JAE	EVAL-PROG	INDC(JPN)-181U			MAR 98	SHIBATA+.EVALUATION FOR JENDL-3.3
HG	201	(N,GAMMA)	1.0-5	2.0+7	JAE	EVAL-PROG	INDC(JPN)-181U			MAR 98	SHIBATA+.EVALUATION FOR JENDL-3.3
HG	201	SPECT (N,G)	1.0-5	2.0+7	JAE	EVAL-PROG	INDC(JPN)-181U			MAR 98	SHIBATA+.EVALUATION FOR JENDL-3.3
HG	201	INELA GAMMA	1.0-5	2.0+7	JAE	EVAL-PROG	INDC(JPN)-181U			MAR 98	SHIBATA+.EVALUATION FOR JENDL-3.3

ELEMENTS	A	QUANTITY	ENERGY MIN	ENERGY MAX	LAB	TYPE	DOCUMENTATION REF	VOL	PAGE	DATE	COMMENTS
HG	201	NONELA GAMMA	1.0-5	2.0+7	JAE	EVAL-PROG	INDC(JPN)-181U			MAR 98	SHIBATA+.EVALUATION FOR JENDL-3.3
HG	201	(N,2N)	1.0-5	2.0+7	JAE	EVAL-PROG	INDC(JPN)-181U			MAR 98	SHIBATA+.EVALUATION FOR JENDL-3.3
HG	201	(N,XN) X>2	1.0-5	2.0+7	JAE	EVAL-PROG	INDC(JPN)-181U			MAR 98	SHIBATA+.EVALUATION FOR JENDL-3.3
HG	201	(N,P)	1.0-5	2.0+7	JAE	EVAL-PROG	INDC(JPN)-181U			MAR 98	SHIBATA+.EVALUATION FOR JENDL-3.3
HG	201	(N,NP)	1.0-5	2.0+7	JAE	EVAL-PROG	INDC(JPN)-181U			MAR 98	SHIBATA+.EVALUATION FOR JENDL-3.3
HG	201	(N,ALPHA)	1.0-5	2.0+7	JAE	EVAL-PROG	INDC(JPN)-181U			MAR 98	SHIBATA+.EVALUATION FOR JENDL-3.3
HG	201	(N,NA)	1.0-5	2.0+7	JAE	EVAL-PROG	INDC(JPN)-181U			MAR 98	SHIBATA+.EVALUATION FOR JENDL-3.3
HG	201	RESON PARAMS	1.0-5	2.0+7	JAE	EVAL-PROG	INDC(JPN)-181U			MAR 98	SHIBATA+.EVALUATION FOR JENDL-3.3
HG	202	ELASTIC	1.0-5	2.0+7	JAE	EVAL-PROG	INDC(JPN)-181U			MAR 98	SHIBATA+.EVALUATION FOR JENDL-3.3
HG	202	DIFF ELASTIC	1.0-5	2.0+7	JAE	EVAL-PROG	INDC(JPN)-181U			MAR 98	SHIBATA+.EVALUATION FOR JENDL-3.3
HG	202	TOT INELAST	1.0-5	2.0+7	JAE	EVAL-PROG	INDC(JPN)-181U			MAR 98	SHIBATA+.EVALUATION FOR JENDL-3.3
HG	202	DIFF INELAST	1.0-5	2.0+7	JAE	EVAL-PROG	INDC(JPN)-181U			MAR 98	SHIBATA+.EVALUATION FOR JENDL-3.3
HG	202	(N,GAMMA)	1.0-5	2.0+7	JAE	EVAL-PROG	INDC(JPN)-181U			MAR 98	SHIBATA+.EVALUATION FOR JENDL-3.3
HG	202	SPECT (N,G)	1.0-5	2.0+7	JAE	EVAL-PROG	INDC(JPN)-181U			MAR 98	SHIBATA+.EVALUATION FOR JENDL-3.3
HG	202	INELA GAMMA	1.0-5	2.0+7	JAE	EVAL-PROG	INDC(JPN)-181U			MAR 98	SHIBATA+.EVALUATION FOR JENDL-3.3
HG	202	NONELA GAMMA	1.0-5	2.0+7	JAE	EVAL-PROG	INDC(JPN)-181U			MAR 98	SHIBATA+.EVALUATION FOR JENDL-3.3
HG	202	(N,2N)	1.0-5	2.0+7	JAE	EVAL-PROG	INDC(JPN)-181U			MAR 98	SHIBATA+.EVALUATION FOR JENDL-3.3
HG	202	(N,XN) X>2	1.0-5	2.0+7	JAE	EVAL-PROG	INDC(JPN)-181U			MAR 98	SHIBATA+.EVALUATION FOR JENDL-3.3
HG	202	(N,P)	1.0-5	2.0+7	JAE	EVAL-PROG	INDC(JPN)-181U			MAR 98	SHIBATA+.EVALUATION FOR JENDL-3.3
HG	202	(N,NP)	1.0-5	2.0+7	JAE	EVAL-PROG	INDC(JPN)-181U			MAR 98	SHIBATA+.EVALUATION FOR JENDL-3.3

ELEMENT S	A	QUANTITY	ENERGY MIN	ENERGY MAX	LAB	TYPE	DOCUMENTATION REF	VOL	PAGE	DATE	COMMENTS
HG	202	(N,ALPHA)	1.0-5	2.0+7	JAE	EVAL-PROG	INDC(JPN)-181U			MAR 98	SHIBATA+.EVALUATION FOR JENDL-3.3
HG	202	(N,NA)	1.0-5	2.0+7	JAE	EVAL-PROG	INDC(JPN)-181U			MAR 98	SHIBATA+.EVALUATION FOR JENDL-3.3
HG	202	RESON PARAMS	1.0-5	2.0+7	JAE	EVAL-PROG	INDC(JPN)-181U			MAR 98	SHIBATA+.EVALUATION FOR JENDL-3.3
HG	204	ELASTIC	1.0-5	2.0+7	JAE	EVAL-PROG	INDC(JPN)-181U			MAR 98	SHIBATA+.EVALUATION FOR JENDL-3.3
HG	204	DIFF ELASTIC	1.0-5	2.0+7	JAE	EVAL-PROG	INDC(JPN)-181U			MAR 98	SHIBATA+.EVALUATION FOR JENDL-3.3
HG	204	TOT INELAST	1.0-5	2.0+7	JAE	EVAL-PROG	INDC(JPN)-181U			MAR 98	SHIBATA+.EVALUATION FOR JENDL-3.3
HG	204	DIFF INELAST	1.0-5	2.0+7	JAE	EVAL-PROG	INDC(JPN)-181U			MAR 98	SHIBATA+.EVALUATION FOR JENDL-3.3
HG	204	(N,GAMMA)	1.0-5	2.0+7	JAE	EVAL-PROG	INDC(JPN)-181U			MAR 98	SHIBATA+.EVALUATION FOR JENDL-3.3
HG	204	SPECT (N,G)	1.0-5	2.0+7	JAE	EVAL-PROG	INDC(JPN)-181U			MAR 98	SHIBATA+.EVALUATION FOR JENDL-3.3
HG	204	INELA GAMMA	1.0-5	2.0+7	JAE	EVAL-PROG	INDC(JPN)-181U			MAR 98	SHIBATA+.EVALUATION FOR JENDL-3.3
HG	204	NONELA GAMMA	1.0-5	2.0+7	JAE	EVAL-PROG	INDC(JPN)-181U			MAR 98	SHIBATA+.EVALUATION FOR JENDL-3.3
HG	204	(N,2N)	1.0-5	2.0+7	JAE	EVAL-PROG	INDC(JPN)-181U			MAR 98	SHIBATA+.EVALUATION FOR JENDL-3.3
HG	204	(N,XN) X>2	1.0-5	2.0+7	JAE	EVAL-PROG	INDC(JPN)-181U			MAR 98	SHIBATA+.EVALUATION FOR JENDL-3.3
HG	204	(N,P)	1.0-5	2.0+7	JAE	EVAL-PROG	INDC(JPN)-181U			MAR 98	SHIBATA+.EVALUATION FOR JENDL-3.3
HG	204	(N,NP)	1.0-5	2.0+7	JAE	EVAL-PROG	INDC(JPN)-181U			MAR 98	SHIBATA+.EVALUATION FOR JENDL-3.3
HG	204	(N,ALPHA)	1.0-5	2.0+7	JAE	EVAL-PROG	INDC(JPN)-181U			MAR 98	SHIBATA+.EVALUATION FOR JENDL-3.3
HG	204	(N,NA)	1.0-5	2.0+7	JAE	EVAL-PROG	INDC(JPN)-181U			MAR 98	SHIBATA+.EVALUATION FOR JENDL-3.3
HG	204	RESON PARAMS	1.0-5	2.0+7	JAE	EVAL-PROG	INDC(JPN)-181U			MAR 98	SHIBATA+.EVALUATION FOR JENDL-3.3
BI	209	(N,XN) X>2	2.0+7	1.5+8	TOH	EXPT-PROG	INDC(JPN)-181U			MAR 98	KIM+.SIG IN FIG.X=3-12
U	233	FRAG NEUTS	2.5-2		KTO	EXPT-PROG	INDC(JPN)-181U			MAR 98	NISHIO+.SIMUL MEAS FF AND PROMPT N

ELEMENT S	A	QUANTITY	ENERGY MIN	ENERGY MAX	LAB	TYPE	DOCUMENTATION REF VOL PAGE DATE	COMMENTS
U	233	FISS YIELD	2.5-2		KTO	EXPT-PROG	INDC(JPN)-181U MAR 98	NISHIO+.SIMUL MEAS FF AND PROMPT N
U	233	FRAG SPECTRA	2.5-2		OSA	EXPT-PROG	INDC(JPN)-181U MAR 98	BABA+.DOUBLE-ENERGY METHOD
U	235	FRAG SPECTRA	2.5-2		OSA	EXPT-PROG	INDC(JPN)-181U MAR 98	BABA+.DOUBLE-ENERGY METHOD
AM	241	FISSION	1.0-1	1.0+4	KTO	EXPT-PROG	INDC(JPN)-181U MAR 98	YAMAMOTO+.THR VAL=3.15+-0.097 BARNS
AM	241	FISSION	1.0-1	1.0+4	KTO	EXPT-PROG	INDC(JPN)-181U MAR 98	KOBAYASHI+.REL U235 FIS
AM	242	FISSION	1.0-1	1.0+4	KTO	EXPT-PROG	INDC(JPN)-181U MAR 98	KOBAYASHI+.REL U235 FIS.FROM META
AM	243	FISSION	1.0-1	1.0+4	KTO	EXPT-PROG	INDC(JPN)-181U MAR 98	KOBAYASHI+.REL U235 FIS
MANY		NONELA GAMMA	1.0-5	2.0+7	JAE	EVAL-PROG	INDC(JPN)-181U MAR 98	SHIBATA+.IMPROVEMENT FOR JENDL-3.2
MANY		(N,ALPHA)	1.3+7	1.5+7	NAG	THEO-PROG	INDC(JPN)-181U MAR 98	KASUGAI+.SYSTEMATICS OF (N,A) SIG
MANY		FISSION	1.0+6	1.0+9	JAE	THEO-PROG	INDC(JPN)-181U MAR 98	FUKAHORI+.SYSTEMATICS OF FIS SIG

I. Electrotechnical Laboratory

A. Quantum Radiation Division

I-A-1 Development of Intermediate Neutron Fluence Standard by Using $^{45}Sc(p,n)^{45}Ti$ Reaction and $^{124}Sb(\gamma)$-Be Source

K. Kudo[1], N. Takeda[1], M. Fujishiro[2], K. Okamoto[3], K. Kobayashi[3]and S. Yoshimoto[3]

For neutron radiation dosimetry in many working environments around nuclear reactors, a significant fraction of the neutron equivalent dose is due to neutrons within the energy range from thermal to 25 keV. Because of the difficulty of producing suitable monoenergetic neutron sources, instruments are rarely calibrated in this energy range and biological data are sparse. Thus calibration fields of monoenergetic neutrons are necessary for this energy range from a few keV to 50 keV. Different techniques are known for producing monoenergetic neutrons in this energy range, such as a radioisotope neutron source of $^{124}Sb(\gamma)$-Be, iron filtered reactor neutron beams and the reaction of $^{45}Sc(p,n)^{45}Ti$.

The radioisotope of ^{124}Sb with a half life of 60.20 days was produced at the Kyoto University Reactor (KUR) and sent to the Electrotechnical Laboratory (ETL) to determine the precise neutron emission rate measured by the manganese bath method[1)] with an uncertainty of ±1%. The energy spectrum from the Sb-Be source with the dimension of $3cm^{D}x3cm^{H}$ was calculated by the MCNP-4 Monte Carlo code[2)]. The 62 % amount of neutrons produced in the source were scattered by Be blanket and gave a continuous spectrum composed by the broad energy part from 0 keV to 22 keV and the higher energy part ranging from 22 keV to 25 keV[3)].

The second source of an iron filtered beam at the B1 experimental facility of KUR was established as a standard source of intermediate neutrons[4)]. We have been performing the intercomparison by using a ^{3}He or H_2 proportional counter with or without a shadow cone with a homogeneous mixture of polyethylene and 10% lithium fluoride. The measurement will be continued by changing the thickness of iron filter to find a adequate condition of the beam intensity.

The third source of $^{45}Sc(p,n)^{45}Ti$ reaction was produced by a Van de Graaff type accelerator at ETL[5)]. The neutron yield of the reaction was determined as a function of the incident proton beam energy using a DC beam with the energy resolution of 2 keV (FWHM). Scandium metal targets with a thickness of 30 $\mu g/cm^2$ were used corresponding to an energy loss of about 2 keV for incident proton energy. The neutron fluence was measured with a calibrated long counter at 0° with respect to the direction of the proton beam. The effect of scattered neutron background was taken into account by placing a shadow cone between the target and the long counter. Other background neutrons contaminated in the field produced around the slit were measured by decreasing the energy of incident protons just below the threshold energy 2.908 MeV of the $^{45}Sc(p,n)^{45}Ti$ reaction.

---

[1] Quantum Radiation Division, Electrotechnical Laboratory

[2] Research Institute for Advanced Science and Technology, Osaka Prefecture University

[3] Research Reactor Institute, Kyoto University

ETL has been doing the calibration of Bonner sphere counters at 24.5 keV for the international intercomparison of intermediate neutron fluence held under the auspices of the Bureau International des Poids et Mesures and would be expected to contribute to establish the international standard.

References

1) K. Kudo, Researches of Electrotechnical Laboratory No.825 (1982).
2) Documentation for CCC-200/MCNP 4.2 Code Package, DLC-105 (1993).
3) N. Takeda, K. Kudo, T. Sugita, M. Fujishiro and K. Okamoto, Proc. Of the Scientific Meeting of the Research Reactor Institute, Kyoto University (1996)67.
4) H. Utsumi, K. Kobayashi et. al., Proc. Of the Scientific Meeting of the Research Reactor Institute, Kyoto University (1996)311.
5) K. Kudo, T. Michikawa et. al., J. Nucl. Sci. Technol., 24 (1987) 684.

I-A-2 SEARCH FOR BOUND STATE M1 TRASITIONS IN ^{208}Pb

H.Ohgaki, T.Noguchi, H.Toyokawa, S.Sugiyama, T.Mikado, K.Yamada, R.Suzuki, T.Ohdaira, N.Sei, and T.Yamazaki

A paper on this subject was presented at International Conference on Nuclear Structure and Related Topics at Dubna, Russia held on Sep.9-13, 1997.

Polarized gamma rays are of interest in the field of nuclear physics, because the real photon has high spin selectivity and a polarized beam assigns an unambiguous parity. Highly polarized gamma rays, Laser Compton Photons (LCPs), have been developed to investigate the substructure of the giant-dipole resonance. The LCP facility employs a conventional Nd:YLF laser with electrons circulating in the electron storage ring TERAS at Electrotechnical Laboratory. The available LCP energy covers from 1 to 40 MeV.[1] By using such LCPs, the nuclear fluorescence experiment to assign the parities of J=1 levels in ^{208}Pb has been started.[2] Completely linear-polarized LCPs of 7.8 MeV with 13% energy spread bombarded an enriched(98.4%) ^{208}Pb target of 8767 mg, 7 mm in diameter and 15 mm long. A pure-Ge detector that has 120% relative detection efficiency has been used to measure the scattered photon at a scattering angle of 90° and 127°. To reduce the pile-up effect from Compton scattering photons from the target, a 4-mm thick lead hardener was placed between the target and the pure-Ge detector. A lead collimator of 50 mm thick was placed in front of the Ge detector and it defined the detector solid angle of 0.85 sr with its entrance window of 40x20 mm^2. The Ge detector was surrounded by lead shield of 20 cm thick which was thick enough because of extremely low background. The incoming photon beam was highly, >90%, linear polarized beam whose polarization axis was changed in 100 seconds interval. The top figure of fig.1 shows the energy spectrum of the elastic scattering photons against the parallel-polarized photons. The bottom one shows that of the elastic scattering photons against the perpendicularly polarized photons. Thus the upper peak shows that this resonance level has the positive parity originated in M1 or E2 transition. On the other hand, the lower peak shows the negative parity originated in E1 transition. This is clear in the asymmetry analysis displayed in figure 2. The E2 and the M1 were separated by the angular distribution of the scatted photons. Generally, an intensity ratio, W(90°)/W(127°), has been commonly used to analyze the angular distribution. Figure 3 shows the measured intensity ratio. Three M1 transitions are newly found at 7.175, 7.207, and 7.243 MeV. Table 1 shows the present results. Furthermore two M1 candidates are found in 6.957 and 7.112 MeV. Three 2^+ levels and sixteen 1^- levels are also observed. The total M1 transition strength of ^{208}Pb is deduced to be 7.14±2 μ_N^2 from 6.8 to 7.3 MeV and this strength exhausts the total strength predicted by the RPA calculation[2] which includes 2p-2h as well as 1Δ–1h configurations. The present M1 strength distribution centers on 7.38 MeV and width of about 1.3 MeV shows excellent agreement with that from the calculation.

References

1)H.Ohgaki et al. , Nucl. Instr. and Meth. A375(1995)602.

2)D.Cha et al., Nucl. Phys. A430, 321 (1984).

3)T.Chapuran et al., Phys. Rev.C, vol.22(1980)1420.

Table 1 Results of $^{206,208}Pb(\gamma_{pol},\gamma)$ experiment. Parentheses indicate tentative assignments.

Energy (MeV)	J^{π}	Γ_0^2/Γ (eV) [a]	Γ_0^2/Γ (eV) [b]	Strength
6.720	1^-	6.46±2.51	7.6±1.5	0.059±0.023 e^2fm^2
6.751	1^-	0.76±0.86		0.007±0.008 e^2fm^2
6.883	(1^-)	3.04±1.72		0.026±0.015 e^2fm^2
6.897	1^-	1.43±1.18		0.012±0.010 e^2fm^2
6.911	(1^-)	2.57±1.58		0.022±0.014 e^2fm^2
6.941	1^-	2.38±1.52		0.020±0.013 e^2fm^2
6.957	(1^+)	2.00±1.40		1.53±1.07 μ_N^2
6.985	1^-	1.24±1.10		0.010±0.009 e^2fm^2
7.020	(1^-)	1.24±1.10		0.010±0.009 e^2fm^2
7.034	1^-	2.28±1.49		0.019±0.012 e^2fm^2
7.044	1^-	2.85±1.67		0.024±0.014 e^2fm^2
7.054	(1^-)	1.52±1.22		0.013±0.010 e^2fm^2
7.062	1^-	13.50±3.63	15.7±2.6	0.11±0.030 e^2fm^2
7.083	1^-	9.03±2.97	8.8±1.5	0.074±0.024 e^2fm^2
7.112	(1^+)	1.14±1.06		0.84±0.77 μ_N^2
7.132	1^-	1.52±1.22		0.012±0.010 e^2fm^2
7.175	1^+	1.05±1.01		0.75±0.73 μ_N^2
7.207	1^+	1.71±1.29		1.2±0.92 μ_N^2
7.243	1^+	2.47±1.55	1.7±0.6	1.7±1.1 μ_N^2
7.280	1^+	1.52±1.22	1.7±0.6	1.1±0.85 μ_N^2
7.300	2^+	1.33±1.14		414±355 e^2fm^4
7.314	2^+	4.09±2.00		1263±618 e^2fm^4
7.332	1^-	26.90±5.13	26.9±4.8	0.21±0.039 e^2fm^2
7.350	(2^+)	0.29±0.53		86.4±220 e^2fm^4
7.549	1^-	1.24±1.10		0.009±0.008 e^2fm^2

a)Normalized to 7.332 MeV level.

b)Data from Ref. 3.

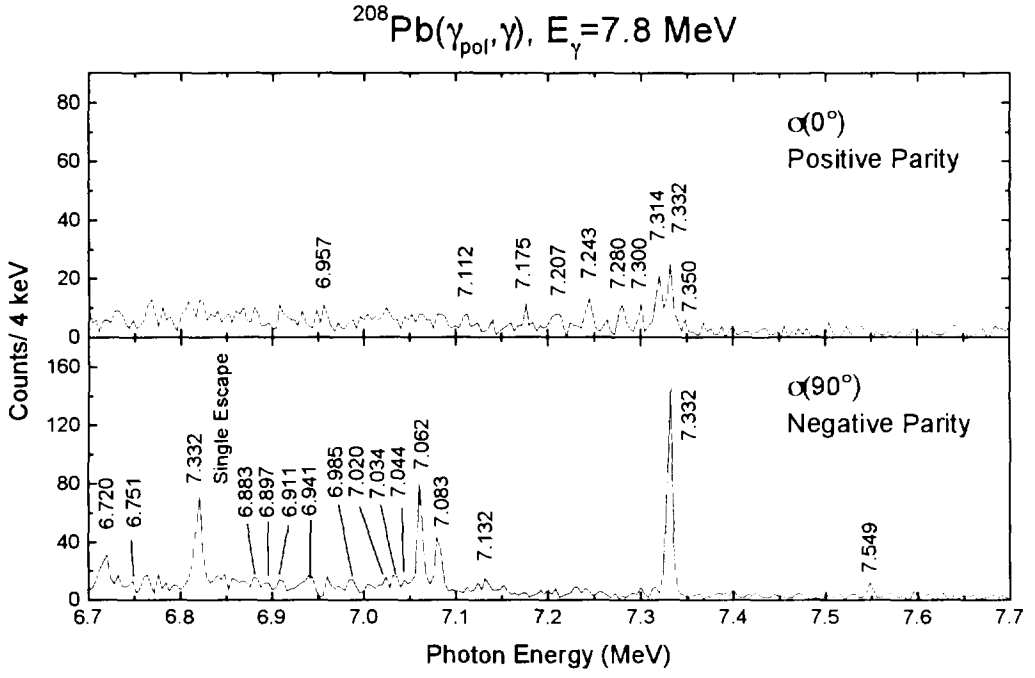

Fig.1 Top figure shows the energy spectrum of the ^{208}Pb(γ_{pol},γ) experiment at the scattering angle of 90° against the parallel-polarized plane, and the bottom figure displays that against the perpendicularly polarized plane.

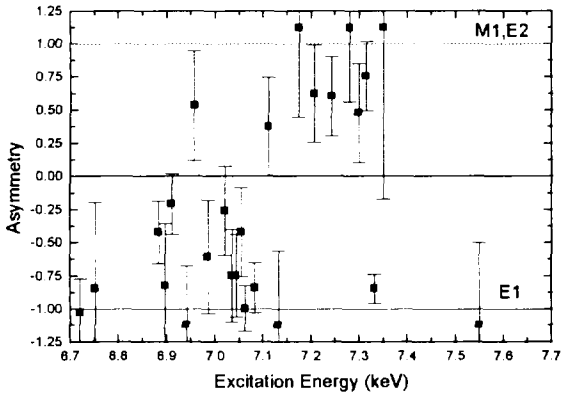

Fig.2 Measured asymmetry for individual peaks in ^{208}Pb(γ_{pol}, γ) experiment.

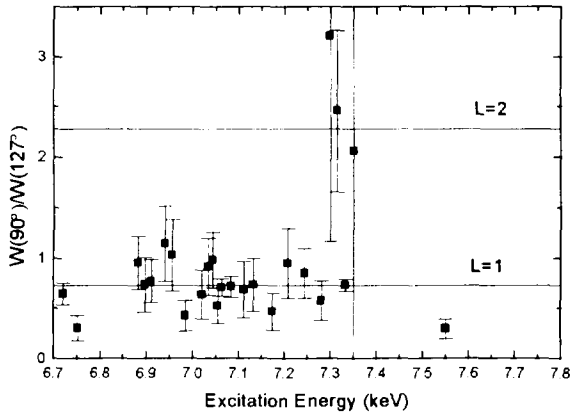

Fig.3 Measured intensity ratio for individual peaks in ^{208}Pb(γ_{pol}, γ) experiment.

II. Japan Atomic Energy Research Institute

A. Nuclear Data Center and Working Groups of Japanese Nuclear Data Committee

II-A-1 Improvement of Gamma-ray Production Data for JENDL-3.2

K. Shibata, S. Igarasi, T. Asamai, M. Mizumoto, M. Igashira,
H. Kitazawa and K. Hida

A paper on this subject was published in J. Nucl. Sci. Technol., **34**, 503 (1997)
with the following abstract:

Gamma-ray production cross sections and spectra have been updated for the latest version of JENDL-3 (JENDL-3.2). Problems of gamma-ray production data contained in the previous version JENDL-3.1 were examined, and they have been mostly resolved in the present work. In the medium-heavy mass region, capture gamma-ray spectra for incident neutron energies below 10 keV were re-calculated with the statistical model taking account of experimentally determined branching ratios for primary transitions. For natural elements, line gamma-rays due to inelastic scattering were explicitly given in JENDL-3.2 up to several MeV. Capture cross sections of some light nuclides were evaluated by considering a p-wave capture behavior indicated by recent measurements. Gamma-ray production data for 66 nuclides have been compiled into JENDL-3.2 in the ENDF-6 format.

II-A-2 Evaluation of Neutron Nuclear Data for Mercury

K. Shibata, T. Fukahori, S. Chiba and N. Yamamuro

A paper on this subject was published in J. Nucl. Sci. Technol., **34**, 1171 (1997)
with the following abstract:

Neutron nuclear data of stable mercury isotopes have been evaluated in the energy range of 10^{-5} eV to 20 MeV. Evaluated quantities are the total, elastic and inelastic scattering, capture, (n,2n), (n,3n), (n,p), (n,α), (n,np), (n,nα) reaction and gamma-ray production cross sections, resonance parameters, and the angular and energy distributions of emitted neutrons and gamma-rays. The evaluation is mainly based on nuclear reaction model calculations. Statistical-model calculation played a significant role in the determination of the reaction cross sections. The evaluated data have been compiled in the ENDF-6 format, and are used for the design study of a mercury target system proposed at the Neutron Science Research Center, JAERI.

II-A-3 Curves and Tables of Neutron Cross Sections in JENDL-3.2

K. Shibata, T. Nakagawa, H. Sugano* and H. Kawasaki*

A paper on this subject was published in JAERI-Data/Code 97-003 (1997) with the following abstract:

Neutron cross sections of 340 nuclei in JENDL-3.2 are shown in graphs and tables. Average values of total, elastic scattering and capture cross sections are also illustrated with 70 energy-group structure. Tabulated are thermal cross sections, 14-MeV cross sections, resonance integrals, Maxwellian- and fission-spectrum average cross sections calculated from JENDL-3.2.

II-A-4 Estimation of Uncertainties in Resonance Parameters of ^{56}Fe, ^{239}Pu, ^{240}Pu and ^{238}U

T. Nakagawa and K. Shibata

A paper on this subject was published in JAERI-Research 97-035 (1997) [in Japanese] with the following abstract:

Uncertainties have been estimated for the resonance parameters of ^{56}Fe, ^{239}Pu, ^{240}Pu and ^{238}U contained in JENDL-3.2. Errors of the parameters were determined from the measurements which the evaluation was based on. The estimated errors have been compiled in the MF32 of the ENDF format. The numerical results are given in tables.

---

* CRC Research Institute, Inc.

II-A-5 Estimation of Covariances of ^{16}O, ^{23}Na, Fe, ^{235}U, ^{238}U and ^{239}Pu Neutron Nuclear Data in JENDL-3.2

K. Shibata, Y. Nakajima, T. Kawano,
Soo Youl OH*, H. Matsunobu and T. Murata

A paper on this subject was published in JAERI-Research 97-074 (1997) with the following abstract:

Covariances of nuclear data have been estimated for 6 nuclides contained in JENDL-3.2. The nuclides considered are ^{16}O, ^{23}Na, Fe, ^{235}U, ^{238}U, and ^{239}Pu, which are regarded as important for the nuclear design study of fast reactors. The physical quantities for which covariances are deduced are cross sections, resolved and unresolved resonance parameters, and the first order Legendre-polynomial coefficient for the angular distribution of elastically scattered neutrons. As for ^{235}U, covariances were obtained also for the average number of neutrons emitted in fission. The covariances were estimated by using the same methodology that had been used in the JENDL-3.2 evaluation in order to keep a consistency between mean values and their covariances. The least-squares fitting code GMA was used in estimating covariances for reactions of which JENDL-3.2 cross sections had been evaluated by taking account of measurements. In nuclear model calculations, the covariances were calculated by the KALMAN system. The covariance data obtained were compiled in the ENDB-6 format, and will be put into the JENDL-3.2 Covariance File which is one of JENDL special purpose files..

* Korea Atomic Energy Research Institute

II-A-6

Development of Libraries for ORIGEN2 Code Based on JENDL-3.2

Kenya SUYAMA
Dept. of Fuel Cycle Safety Research, JAERI, Tokai-mura, Ibaraki-ken, 319-11, JAPAN
e-mail: kenya@cyclone.tokai.jaeri.go.jp

Jun-ichi KATAKURA
Nuclear Data Center, JAERI, Tokai-mura, Ibaraki-ken, 319-11, JAPAN
e-mail: katakura@cracker.tokai.jaeri.go.jp

Makoto ISHIKAWA
O-arai Engineering Center, PNC, O-arai-machi, Ibaraki-ken, JAPAN
e-mail:ishikawa@oec.pnc.go.jp

Yasushi OHKAWACHI
O-arai Engineering Center, PNC, O-arai-machi, Ibaraki-ken, JAPAN
e-mail: okawachi@oec.pnc.go.jp

ORIGEN2 code[1] is one of the most widely used burnup codes for many purposes. The advantage of using ORIGEN2 is that it has a variety of data libraries for various reactor systems. However, the libraries are based on obsolete design of reactors and old nuclear data libraries. To overcome these problems, JNDC launched the project to make libraries of ORIGEN2 code based on the current reactor design using JENDL-3.2. The aim of making these libraries is to evaluate assembly averaged isotopic composition as correctly as possible.

The main work in this fiscal year was to make libraries of LWR and FBR. For LWR, three PWR libraries of 17 × 17 fuel assembly was prepared. Also, nine libraries for BWR STEP-1, 2 and 3 fuel assembly were developed. To carry out this work, SWAT[2] was used. For verification of PWR libraries, one of the latest PIE was analyzed. This analysis showed improved results for U and Pu isotopes using our new library. For FBR, libraries for eight types of cores were constructed using new code system[3]. The comparison using new and old libraries for FBR revealed that some isotopes had large deviations that resulted from the difference of source of nuclear data and the collapsing neutron spectrums. The outline of our activities was presented at the 1997 Symposium on Nuclear Data[3].

Current status of these libraries are under evaluation. After extensive tests performed, these libraries will be hopefully distributed for use in many fields of nuclear engineering.

References

[1] Croff, A.G.: *ORNL-5621*(1980).

[2] Suyama,K. et al: *JAERI-Data/Code 97-047*, (1997)(in Japanese).

[3] To be published as JAERI-Conf(1998).

II-A-7 Status of JENDL Intermediate Energy Nuclear Data File

T. Fukahori, S. Chiba, N. Kishida, M. Kawai, Y. Oyama and A. Hasegawa

A paper on this subject will be published in Proc. of the International Conference on Nuclear Data for Science and Technology, May 19-24, 1997, Trieste, Italy with the following abstract.

The JAERI Nuclear Data Center has started evaluation work in cooperation with Japanese Nuclear Data Committee (JNDC) to produce evaluated intermediate energy nuclear data files which are JENDL High Energy File, JENDL PKA/KERMA File and JENDL Photonuclear Data File. JENDL High Energy File will include nuclear data for proton- and neutron- induced reactions up to 2 GeV. For photonuclear reaction data up to 140 MeV, JENDL Photonuclear Data File is provided for applications such as electron accelerator shielding and radiation therapy. JENDL PKA/KERMA File is generated to supply PKA spectra, damage energy spectra, DPA (displacement per atom) cross sections and kerma factors by neutron-induced reactions up to 50 MeV for estimation of radiation damage. The present status of these files is reported in this paper.

II-A-8 Status of Nuclear Data Evaluation for JENDL Photonuclear Data File

T. Fukahori and JNDC (Photonuclear Data Evaluation WG)

A paper on this subject will be published in Proc. of the Third Specialists' Meeting on Shielding Aspects of Accelerator, Targets and Irradiation Facilities (SATIF-3), May. 12 - 13, 1997, Tohoku University, Sendai, Japan with the following abstract.

For γ-ray induced reaction data up to 140 MeV, the JENDL Photonuclear Data File is provided for applications such as electron accelerator shielding and radiation therapy. The file will include the photonuclear reaction data for 29 elements (50 isotopes) from H-2 to U-238. The photon absorption cross section is evaluated with the giant dipole resonance model and quasi-deuteron model, and the decaying processes are estimated with the statistical model with preequilibrium correction by using MCPHOTO and ALICE-F codes. The evaluation work is now in a final stage. In this paper, the present status of the Photonuclear Data File is reviewed.

II-A-9 Systematics of Fission Cross Sections at the Intermediate Energy Region

T. Fukahori, O. Iwamoto and S. Chiba

The fission cross section of actinide nuclei is one of the important physical quantities for radioactive waste transmutation. Calculation tools for this quantity in the intermediate energy region are still under development, except some codes such as ALICE and HETC. We have developed a semi-empirical formula for proton-induced fission cross section, which has rather more experimental data than the other particle induced cross sections. On the other hand, neutron-induced fission cross sections in the intermediate energy region have been systematically measured at Gatchina (Russia) and Los Alamos National Laboratory (U.S.). This report shows the semi-empirical formula previously developed has been expanded for neutron-, proton- and photon-induced fission cross sections simultaneously and the formula succeeded to explain most of experimental data.

The Z- and A-independent parameters, $q_{i,j}$, has been fit by using experimental data for 29 isotopes from Ag to ^{243}Am with following formula;

$$P_{fis}(Z, A, E) = p_1 \cdot [1 - \exp\{-p_3(E - p_2)\}]$$
$$p_i = \exp(q_{i,1} + q_{i,2}x) \qquad (i = 1,2,3, \quad x = Z^2 / A)$$

where P_{fis} is fission cross section fraction to total reaction cross section ($=\sigma_{fis}/\sigma_R$)、Z and A are atomic and mass number of compound nuclei, and E is excited energy. The fitting results are shown in Fig.1 and Table 1, and the "best-fit" parameters have a trend of good linearity. These results can derive that neutron-, proton- and photon-induced fission cross section can be explained by only one formula. This formula can give not only the systematics for fission cross section at a certain energy point but also the shapes of excite function. Using this formula make possible to estimate the fission cross section for the nuclei for which few experimental data exist.

Table 1 Results of parameter fitting.

	p_1	p_2	p_3
$q_{i,1}$	-29.3156	27.0703	-50.4533
$q_{i,2}$	0.807776	-0.698254	1.38907

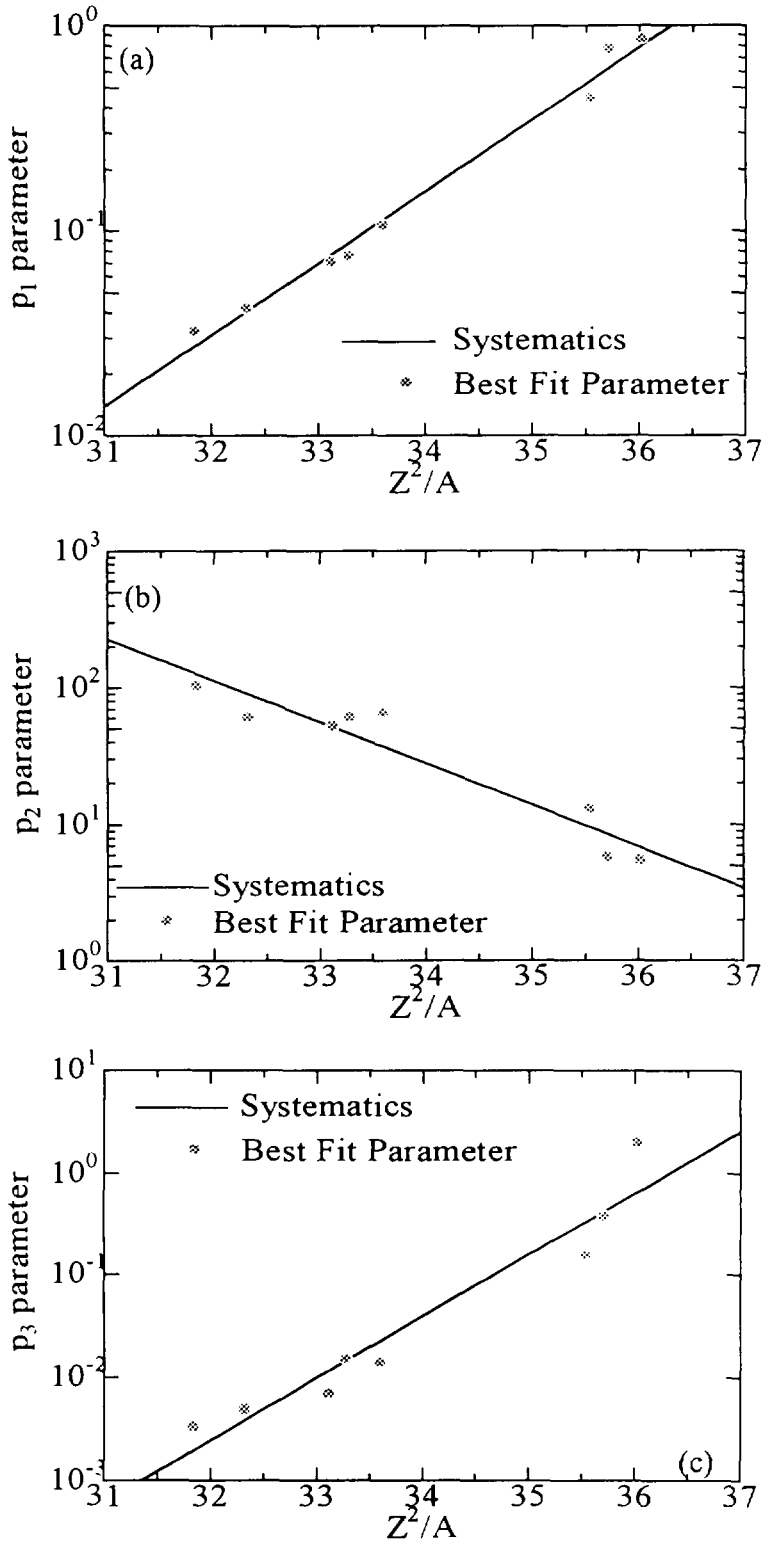

Fig. 1 Fitting results of systematics (solid lines) and "best fit" parameters, which were obtained by directly fitting to experimental data (closed circles) for p_1 (a), p_2 (b) and p_3 (c) parameters.

B. Department of Chemistry and Fuel Research

II-B-1

Conversion Electron Measurements in the ^{127}Ce and ^{127}La β-Decay

H.Iimura, S.Ichikawa, M.Oshima, T.Sekine, J.Katakura, N.Shinohara,
M.Magara, A.Osa, M.Asai, M.Miyaji[1] and H.Yamamoto[2]

We have studied the level scheme of ^{127}La through the β-decay of ^{127}Ce ($T_{1/2}$=31 s) to clarify mainly the structure of low-spin levels. The preliminary results of gamma-ray measurements have already been reported[1]. To obtain internal conversion coefficients we measured electron spectra. The experiments were performed by using the on-line mass separator at the tandem accelerator facility in JAERI. The ^{127}Ce nucleus was produced by the reaction ^{nat}Mo(^{35}Cl,pxn)^{127}Ce with 185-MeV ^{35}Cl beam and mass-separated electromagnetically from other reaction products. A simultaneous measurement of electrons and γ-rays was made with Si(Li) and HPGe detectors. From the present measurements, multipolarities of some transitions have been determined and information on parities of low-lying levels has been obtained. Preliminary level scheme of ^{127}La has been compared with those previously reported. Conversion electron measurements in the β-decay of daughter nucleus, ^{127}La were also made. Further analysis is now in progress.

References

[1] H.Iimura *et al.*, *Proc. of the 9th Int. Symp. on Capture Gamma-Ray Spectroscopy and Related Topics (Springer, 1997) 297*

[1]Toshiba Ltd.
[2]Department of Nuclear Engineering, Nagoya University

III. Kyoto University

A. Research Reactor Institute

III-A-1

Fission Cross Section Measurements of Am-241 between 0.1 eV and 10 keV with Lead Slowing-down Spectrometer and at Thermal Neutron Energy

Shuji Yamamoto[1], Katsuhei Kobayashi[1], Mitsuharu Miyoshi[2*], Itsuro Kimura[2], Ikuo Kanno[2], Nobuo Shinohara[3], and Yoshiaki Fujita[1]

1 Research Reactor Institute, Kyoto University
Kumatori-cho, Sennan-gun, Osaka 590-04, Japan
2 Department of Nuclear Engineering, Kyoto University
Yoshida-honmachi, Sakyo-ku, Kyoto 606-01, Japan
** Present address: GE and Yokogawa Medical System Inc.*
4-chome, Asahigaoka, Hino-shi, Tokyo 191, Japan
3 Department of Radioisotopes, Japan Atomic Energy Research Institute
Tokai-mura, Naka-gun, Ibaraki 319-11, Japan

A paper on this subject was published in Nuclear Science and Technology, Vol.126, No.2, 201-212 (1997) with the following abstract.

Making use of back-to-back type double fission chambers and a lead slowing-down spectrometer coupled to an electron linear accelerator, the cross section for the ^{241}Am(n,f) reaction has been measured relative to that for the ^{235}U(n,f) reaction in the energy range from 0.1 eV to 10 keV. To avoid the interference between the ^{241}Am and the ^{235}U resonances, the fission cross section below 1 keV was measured relative to the ^{10}B(n, α) reaction with a BF_3 counter, and the result obtained was normalized to the absolute value by the ^{235}U reference data between 200 eV and 1 keV. The measured result has been compared with (1) the evaluated nuclear data contained in the ENDF/B-VI and JENDL-3.2 libraries, and (2) the existing experimental data, with the evaluated and measured data being broadened using the energy resolution function of the spectrometer.

There is general agreement between the evaluated data and the present measurement, although some discrepancies are found in the energy region where the cross section shapes show a pronounced structure. The JENDL-3.2 data are underestimated by a factor in the range 1.2 to 2.3 between 22 and 140 eV, while the more recently measured data by Dabbs et al. and the evaluated data in ENDF/B-VI are in good agreement with the measurement within the uncertainties. In the energy range from 1 to 10 keV, the present result is 15 to 18 % higher than the evaluations and the Dabbs' data. Some of the earlier experimental data which were measured over part of the relevant energy region are not always in agreement with the present measurement.

The fission cross section for thermal neutrons was also measured in a pure Maxwellian neutron spectrum field with the double fission chambers. The derived result at 0.0253 eV is 3.15 $\pm$ 0.097 b, which is obtained relative to the reference value of 586.2 b for the ^{235}U(n,f) reaction. The ENDF/B-VI data is in good agreement with the present measurement, while the JENDL-3.2 value is lower by 4.2 %. The ratios of the earlier experimental data to the present value are distributed between 0.89 and 1.02.

III-A-2 Measurement of Fission Cross Sections for Nuclear Transmutation on Am-241, Am-242m and Am-243 Using Lead Slowing-down Spectrometer

Katsuhei Kobayashi[1], Shuji Yamamoto[1], Tetsuya Kai[1], Yoshiaki Fujita[1], Itsuro Kimura[2], Mitsuharu Miyoshi[2], Ikuo Kanno[2], Toshio Wakabayashi[3], Yasushi Ohkawachi[3], Shigeo Ohki[3] and Nobuo Shinohara[4]

1 Research Reactor Institute, Kyoto University
Kumatori-cho, Sennan-gun, Osaka, 590-04 Japan
2 Department of Nuclear Engineering, Kyoto University
Yoshida-honmachi, Sakyo-ku, Kyoto, 606-01 Japan
3 Power Reactor & Nuclear Fuel Development Corporation
Narita, O-arai, Ibaraki, 311-13 Japan
4 Japan Atomic Energy Research Institute
Tokai-mura, Naka-gun, Ibaraki, 319-11 Japan

A paper on this subject was presented at the International Conference on Future Nuclear Systems, Global '97 on October 5-10, 1997, Yokohama, Japan and published in the Proceedings of the Conference, Vol.2, 784-788 (1997) with the following abstract.

Making use of a lead slowing-down spectrometer coupled to a 46 MeV electron linear accelerator and a back-to-back type double fission chamber, the fission cross sections of Am-241, Am-242m and Am-243 have been measured relative to that of U-235 from 0.1 eV to 10 keV with the energy resolution of about 40 % full width at half maximum. Each of the measured result has been compared with (1) the evaluated nuclear data in ENDF/B-VI and JENDL-3.2, and (2) the existing experimental data, for which the evaluated and the experimental data were broadened by the energy resolution function of the spectrometer.

III-A-3

Measurement of the ^{243}Am(n,f) Cross Section Between 0.1 eV and 10 keV Using Lead Slowing-down Spectrometer

Katsuhei Kobayashi[1], Tetsuya Kai[1], Shuji Yamamoto[1], Yoshiaki Fujita[1]
Itsuro Kimura[2] and Nobuo Shinohara[3]

1 Research Reactor Institute, Kyoto University
Kumatori-cho, Sennan-gun, Osaka 590-04, Japan
2 Department of Nuclear Engineering, Kyoto University
Yoshida-honmachi, Sakyo-ku, Kyoto 606-01, Japan
3 Department of Radioisotopes, Japan Atomic Energy Research Institute
Tokai-mura, Naka-gun, Ibaraki 319-11, Japan

A paper on this subject was presented at the International Conference on Nuclear Data for Science and Technology, on May 19-24, 1997, Trieste Italy.

Making use of back-to-back type double fission chambers and a lead slowing-down spectrometer coupled to an electron linear accelerator, the fission cross section for the ^{243}Am(n,f) reaction has been measured relative to that for the ^{235}U(n,f) reaction in the energy range from 0.1 eV to 10 keV. The measured result has been compared with the evaluated nuclear data in ENDF/B-VI and JENDL-3.2, whose evaluated data were broadened by the energy resolution function of the spectrometer. General agreement is seen between the evaluated data and the measurement except that the ENDF/B-VI data are lower in the range from 15 to 60 eV and that the JENDL-3.2 data seem to be lower above 100 eV. The experimental data by Wisshak and Kappeler and by Knitter and Budtz-Jφrgensen are in general agrrement with the present measurement in the relevant energy region. However, the data by Seeger are considerably higher.

III-A-4 Fission Cross Section Measurement of Am-242m using Lead Slowing-down Spectrometer

Tetsuya Kai[1], Katsuhei Kobayashi[1], Shuji Yamamoto[1], Yoshiaki Fujita[1], Itsuro Kimura[2], Yasushi Ohkawachi[3] and Toshio Wakabayashi[3]

1 *Research Reactor Institute, Kyoto University Kumatori-cho, Sennan-gun, Osaka 590-04, Japan*
2 *Department of Nuclear Engineering, Kyoto University Yoshidahonmachi, Sakyo-ku, Kyoto 606-01, Japan*
3 *Power Reactor and Nuclear Fuel Development Corporation 4002 Narita, O-arai machi, Ibaraki, 311-13, Japan*

A paper on this subject was presented at the 1997 Symposium on Nuclear Data at Tokai-mura, JAERI held on Nov. 27-28, 1997.

By making use of double fission chamber and lead slowing-down spectrometer coupled to an electron linear accelerator, fission cross section for the ^{242m}Am(n,f) reaction has been measured relative to that for the ^{235}U(n,f) reaction in the energy range from 0.1 eV to 10 keV. The measured result was compared with the evaluated nuclear data appeared in ENDF/B-VI and JENDL-3.2, of which evaluated data were broadened by the energy resolution function of the spectrometer. Although the JENDL-3.2 data seem to be a little smaller than the present measurement, good agreement can be seen in the general shape and the absolute values. The ENDF/B-VI data are larger more than 50 % than the present values above 3 eV.

B. Department of Nuclear Engineering

III-B-1 Multi-parametric Measurement of Prompt Neutrons and Fission Fragments for $^{233}U(n_{th},f)$

K. Nishio, I. Kimura, M. Nakashima and Y. Nakagome[1]

A paper on this subject was submitted to J. Nucl. Sci. and Technol. for publication [1].

Simultaneous measurement of fission fragments and prompt neutrons for $^{233}U(n_{th},f)$ was carried out with the system reported previously [2][3]. The results determined the neutron multiplicity and emission energy as a function of fragment mass and total kinetic energy.

The measurement was carried out using the slow neutrons from the Kyoto University Reactor. The experimental arrangement is shown in Fig. 1. In the vacuum chamber, the ^{233}U target and fragment detectors were mounted. The kinetic energy of fission fragment 1 (FF1) was determined by using a silicon surface barrier detector (SSBD). The energy of FF2 was obtained from the time difference between the signals from the SSBD and a parallel plate avalanche counter (PPAC). Neutron emitted from the FF1 was detected with a NE213 and the energy was determined by the TOF method, for which the start signal was triggered by the SSBD too.

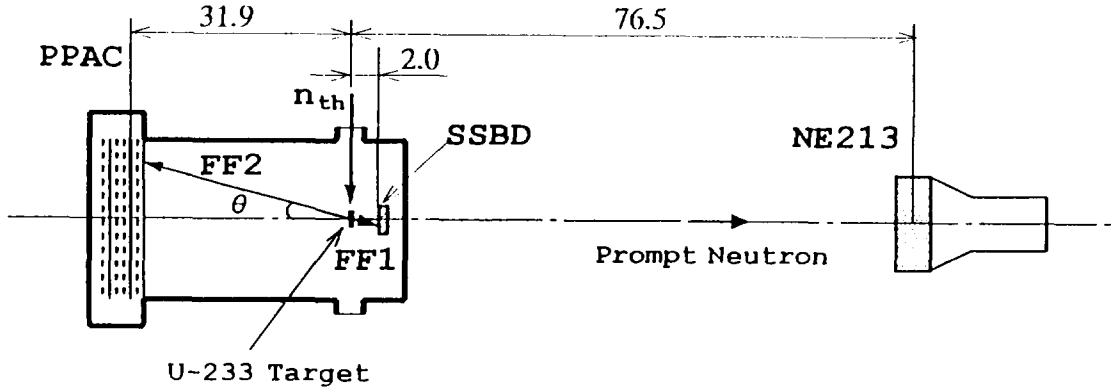

Fig. 1 Experimental arrangement for the simultaneous measurement of fission fragments and prompt neutron.

1. Research Reactor Institute, Kyoto University

The average neutron energy in the fragment center-of-mass system as a function of fragment mass, $\overline{\eta}(m^*)$, is shown in Fig. 2. Also shown is the mass yield curve obtained in this measurement. It is evident that (1) the $\overline{\eta}(m^*)$ is approximately symmetrically distributed about the equal-mass division of the fissioning nucleus, and the minimum values appear at 95 and 145 u, and (2) the neutron energy from the symmetric and very asymmetric fission fragments reaches to about 1.8 MeV. Figure 3(a) shows the average neutron multiplicity from the specified fragment, $\overline{\nu}(m^*)$, and Fig. 3(b) the total neutron multiplicity, $\overline{\nu}^{tot}(m^*)$. Present data are compared to the results by Apalin *et al.* [4] (dotted curve). The interesting aspect is the marked enhancement of the $\overline{\nu}^{tot}(m^*)$ in the symmetric fission. It suggests that the total deformation energy of the system at the scission point is quite large. The saw-toothed shape of $\overline{\nu}(m^*)$ sharply contrasts with the $\overline{\eta}(m^*)$ in Fig. 2. The difference is attributed to the level density parameter of fragments, which is affected by the shell-effects and is expressed by the shell-energy correction. The fragment with $m^* \approx 130$ u is close to the nucleus with double-magic number, ^{132}Sn, and the fragment with $m^* \approx 80$ is close to ^{78}Ni, and thus the level density parameters of these fragments are very low. This is the reason for the experimental evidence that these fragments, which have rather low excitation energy, emit neutrons with high energy.

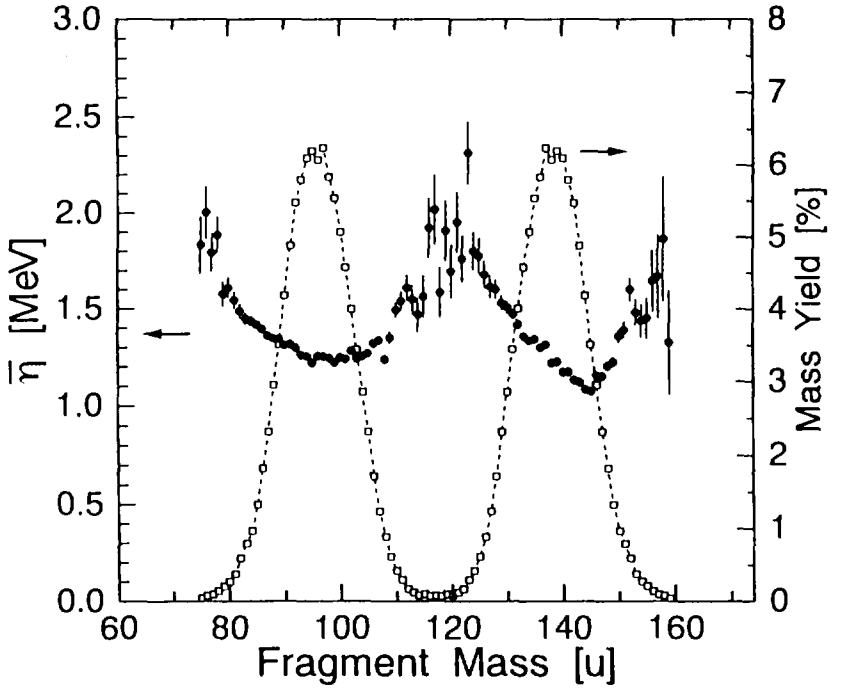

Fig. 2 Average neutron energy as a function of fragment mass for $^{233}U(n_{th},f)$. Mass yield curve obtained in this measurement is also indicated.

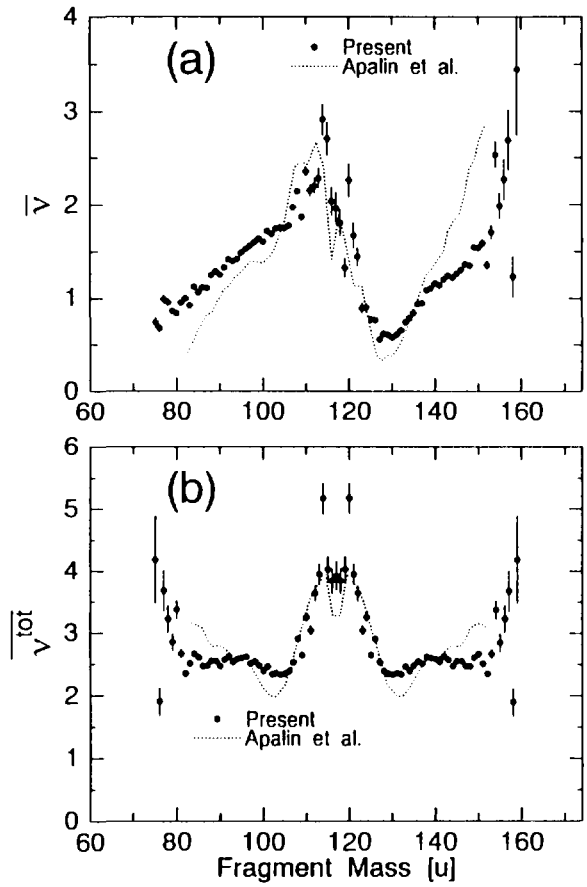

Fig. 3 (a) Average neutron multiplicity. (b) Average total neutron multiplicity. The dotted curve is the data in Ref. [4].

References :

[1] K. Nishio, M. Nakashima, I. Kimura and Y. Nakagome, submitted to J. Nucl. Sci. and Technol.

[2] K. Nishio, H. Yamamoto, I. Kimura and Y. Nakagome, Nucl. Instrum. Meth. A385 (1997) 171.

[3] K. Nishio, Y. Nakagome, H. Yamamoto and I. Kimura, Nucl. Phys. A, accepted for publication.

[4] V.F. Apalin *et al.*, Nucl. Phys. **71** (1965) 553.

IV. Kyushu University

A. Department of Energy Conversion Engineering

IV-A-1 Partial-Wave Analysis with the Optical Model for the Resolved and Unresolved Resonance Regions of ^{56}Fe

T. Kawano and F. H. Fröhner*

A paper on this subject was published in *Nucl. Sci. Eng.*, **127**, p.130, 1997, and partly in the Proc. the First Internet Symposium on Nuclear Data, JAERI, Tokai, 1996, p.257 with the following abstract:

We have studied optical model fits to total neutron cross sections of ^{56}Fe using the accurate data base existing in the resolved and unresolved resonance region. Averages over resolved resonances were calculated from resonance parameters in Reich-Moore (reduced R matrix) approximation with Lorentzian weighting. Optical potential parameters were obtained for the s-, p-, and d-waves that reproduce the smoothed cross sections in the resolved resonance region. The p-wave optical potential was found to differ from the s-wave potential. When the appropriate higher angular momentum contributions are added, the average total cross sections can be fitted quite well, from the resolved resonance region all the way up to 20 MeV.

* Forschungszentrum Karlsruhe, Institut für Neutronenphysik und Reaktortechnik

IV-A-2 Covariance Evaluation System

T. Kawano and K. Shibata**

A paper on this subject was published in JAERI-DATA/Code, 97-037, with the following abstract:

A covariance evaluation system for the evaluated nuclear data library was established. The parameter estimation method and the least squares method with a spline function are used to generate the covariance data. Uncertainties of nuclear reaction model parameters are estimated from experimental data uncertainties, then the covariance of the evaluated cross sections is calculated by means of error propagation. Computer programs ELIESE-3, EGNASH4, ECIS, and CASTHY are used. Covariances of ^{238}U reaction cross sections were calculated with this system.

** Japan Atomic Energy Research Institute

IV-A-3 Application of a Client-Server Model to the Evaluated Nuclear Data Libraries

T. Kawano, O. Sakai, and H. Nakashima

A paper on this subject was partly presented at the 1996 Symposium on Nuclear Data, and published in JAERI-Conf, 97-005, p.307, and published in Engineering Science Reports, Kyushu University, **19**, 317 (1997) with the following abstract:

A nuclear data server which transmits the evaluated nuclear data libraries through network is proposed. The evaluated nuclear data are provided by means of TCP/IP, and client programs can receive the nuclear data with the socket library. Some examples with a prototype server program are demonstrated, the first is a nuclear data retrieval program which allows users to extract data from the nuclear data library, and the second is an access to the nuclear data library from the existent nuclear data process code.

IV-A-4 Measurement of Helium Production Cross Sections of Stainless Steels for 14 MeV Neutrons

Y. Takao, Y. Kanda, Y. Uenohara, T. Takahashi, S. Itadani,
T. Iida*, and A. Takahashi*

A paper on this subject was published in Journal of Nuclear Science and Technology, Vol.34, No.1, 1-4(1997) with the following abstract:

Helium production cross sections of the austenitic stainless steels, Type 316 stainless steel, JPCA, and JPCA2, and the ferritic / martensitic stainless steels, HT-9, and JFMS have been measured for 14.5 MeV neutrons, employing a helium accumulation method. The measured effective cross sections range from 52 to 59 mb with ±8% error and have been compared with the composite values which are calculated from measured or estimated He production cross sections for individual constituent elements. The measured effective cross sections agree well with the composite cross sections. The contributions from constituent elements to the composite cross sections were compared. As a result, the comparison shows that the carbon content of the stainless steel has a significant effect on the He production rate.

* Department of Nuclear Engineering, Osaka University

IV-A-5

Measurement of Proton-Induced Helium Production Cross Sections for Aluminum and Nickel below 16MeV

Y. Takao, Y. Kanda, H. Hashimoto, K. Yamasaki, K. Yamaguchi, T. Yonemoto,
M. Miwa, H. Etoh, and K. Nagae

A paper on this subject was published in Journal of Nuclear Science and Technology, Vol.34, No.2, 109-115(1997) with the following abstract:

Proton-induced He production cross sections, (p,He), for Al and Ni have been measured up to 16 MeV by using a He accumulation method.

The reliability of the present experiment was confirmed by performing three kinds of experiments for the Al(p,He). The sample structure or the manner of measuring the number of bombarding protons differs in each experiment. A comparison of their results shows that it is valid to install an Al sample in a Faraday cup for determination of the absolute number of incident protons and to sandwich a sample sheet by two Au foils to catch outgoing α-particles from the sample surface layer for measuring the all He produced in the sample.

IV-A-6

Measurement of Helium Production Cross Sections of Iron for d-T Neutrons by Helium Accumulation Method

Y. Takao, Y. Kanda, K. Nagae, T. Fujimoto, and Y. Ikeda*

A paper on this subject was presented at the 1996 Symposium on Nuclear Data, and published in JAERI-Conf 97-005, p.159(1997) with the following abstract:

Helium production cross sections of Iron were measured by helium accumulation method for neutron energies from 13.5 to 14.9 MeV. Iron samples were irradiated with FNS, an intense d-T neutron source of JAERI. As the neutron energy varies according to the emission angle at the neutron source, the samples were set around the neutron source and were irradiated by neutrons of different energy depending on each sample position. The amount of helium produced in a sample was measured by Helium Atoms Measurement System at Kyushu University. The results of this work are in good agreement with other experimental data in the literature and also compared with the evaluated values in JENDL-3.

---

* Department of Reactor Engineering, Japan Atomic Energy Research Institute

IV-A-7 Evaluation of Neutron Cross Sections of Carbon-12 for energies up to 80 MeV

M. Harada, Y. Watanabe, S. Chiba*, and T. Fukahori*

A paper on this subject was published in *J. Nucl. Sci. and Technol.* 34, 116 (1997) with the following abstract:

We have evaluated the cross sections of ^{12}C for neutrons up to 80 MeV, paying more attention to the intermediate energy range above 20 MeV. For energies below 20 MeV, the evaluated data of JENDL-3.2 were adopted with some modifications. In the energy range above 20 MeV, total cross section and its covariance matrix were evaluated using a generalized least-squares method with available experimental data. The spherical optical model was used to evaluate reaction and elastic scattering cross sections. Inelastic scattering to the first 2^+ state was calculated based on the DWBA. The optical potentials used in these calculations were obtained by means of the microscopic folding model based on the Jeukenne-Lejeune-Mahaux theory. Double-differential emission cross sections for neutron, proton, deuteron, triton, ^3He and alpha-particle and other heavier products were calculated using the Monte-Carlo method by which three-body simultaneous breakup process and two-body sequential decay process were taken into account in $n+^{12}C$ multibody breakup reactions. Kerma factors calculated from the evaluated cross sections were also compared with measurements and other evaluations.

*Japan Atomic Energy Research Institute

IV-A-8 Development of a system of measuring double-differential cross sections for proton-induced reactions

M. Harada, Y. Watanabe, K. Sato, and S. Meigo*

A paper on this subject was published in JAERI-Conf, 97-005, p.240 with the following abstract:

We report the present status of a counter telescope and a data acquisition system which are being developed for the measurement of double-differential cross sections of all light-charged particles emitted from proton-induced reactions on ^{12}C at incident energies less than 90 MeV. The counter telescope consists of an active collimator made of a plastic scintillator, two thin silicon ΔE-detectors and a CsI(Tl) E-detector with photo-diode readout. Signals from each detector are processed using the data acquisition system consisting of the front-end electronics (CAMAC) and two computers connected with the ethernet LAN: a personal computer as the data collector and server, and a UNIX workstation as the monitor and analyzer.

The above-mentioned detector system has recently been tested using the $\alpha+^{12}C$ reaction at an incident energy of 50 MeV at TIARA (Takasaki, JAERI). The relation between energy and light output for the CsI(Tl) scintillator was measured using emitted light particles (proton, deuteron, triton and alpha particle).It was also found it possible to detect heavier products such as $^{6,7}Li$ and ^7Be using two thin silicon ΔE-detectors. The detector system will be used for an experiment of proton-induced reactions for energies of 45 to 90 MeV which is planned from 1998 at TIARA.

*Japan Atomic Energy Research Institute

IV-A-9 Semi-classical distorted wave model for multistep direct (N,N'x) reactions at intermediate energies

Y. Watanabe, M. Higashi, H. Shinohara, M. Kawai*, and M. Kohno**

A paper on this title was presented at Int. Conf. on Nuclear Data for Science and Technology, May 19-24, 1997, Trieste, Italy with the following abstract:

The Semi-Classical Distorted Wave (SCDW) model has been proposed and developed to describe the multistep direct (MSD) process in preequilibrium nuclear reactions (1). The model is based on the DWBA series of the T-matrix, a local semiclassical approximation of distorted waves, the eikonal approximation to the Green functions describing propagation of the intermediate nucleons, and the local-density Fermi gas model of the nucleus. Recently, the SCDW model has been extended so as to take into account the leading three MSD steps. Using the extended SCDW model, we have analyzed preequilibrium angular distributions of nucleon-induced nucleon-emission (N,N'x) reactions at intermediate energies: *e.g.*, ^{58}Ni(p,p'x) at 65 to 200 MeV and ^{90}Zr(p,p'x) reactions at 160 MeV. The SCDW calculations with no adjustable parameter are in good agreement with the experimental angular distributions, except at very small and large angles. For the SCDW analysis, the contribution from higher order steps, the medium effect on nucleon-nucleon interactions, and the effect of the non-locality correction to distorting potentials are discussed. Moreover, comparisons with other models are made with attention to the step-wise MSD contributions to calculated angular distributions. The use of the simple degenerate Fermi-gas model are resposible for the discrepancies seen at very small and large angles. Finally, we propose a possible approach to treat more realistic nuclear wave functions within the framework of the SCDW model.

After the conference, we have carried out a preliminary calculation of ^{90}Zr(p,p') at 160 MeV using the above-mentioned new approach with the Wigner transform of one-body mixed density. Single-particle wave functions in a harmonic oscillator potential were used instead of those given by the local-density Fermi-gas model. As a result, it was found that the underestimation seen at backward angles is improved well. A further calculation with the Woods-Saxson potential is now in progress. The result with this new approach was partly presented at the 1997 Symp. on Nuclear Data, Nov. 27-28, 1997, JAERI, Tokai, Japan as a paper entitled "Improvements on semi-classical distorted wave model".

References:

(1) Y. L. Luo and M. Kawai, Phys. Rev. C **43**, 2367 (1991); M. Kawai and H.A. Weidenmüller, Phys. Rev. C **45**, 1856 (1992); Y. Watanabe and M. Kawai, Nucl. Phys. **A560**, 43 (1993); M. Kawai, Y. Watanabe and H. Shinohara, acta physica Slovaca **45**, 693 (1995).

*Department of Physics, Kyushu University
** Kyushu Dental College

IV-A-10 Continuum (p,xp) spectra at 14.1 and 26 MeV

Y. Watanabe, S. Yoshioka, M. Harada, K. Sato, Y. Nakao, H. Ijiri,
S. Chiba*, T. Fukahori*, S. Meigo*, M. Iwamoto*, and N. Koori**

A paper on this title was presented at Int. Conf. on Nuclear Data for Science and Technology, May 19-24, 1997, Trieste, Italy with the following abstract and the related work was also published in JAERI-Conf, 97-005, p. 301.

Double differential cross sections of (p,xp) reactions on several medium-heavy nuclei (^{54,56}Fe, ^{60}Ni, ^{90}Zr, and ^{93}Nb) were measured at incident energies of 14.1 and 26 MeV using tandem Van de Graaf accelerators at Kyushu University and Japan Atomic Energy Research Institute (JAERI), respectively. A ΔE-E Si-detector counter telescope with an active collimator consisting of an NE102A plastic scintillator was used in the measurements. The active collimator operates as a veto detector to reduce the continuum background component due to the edge-penetration which makes it difficult to measure (p,p') spectra at small angles.

The data of two targets (i.e., ^{56}Fe and ^{93}Nb) were analysed together with the (n,xn) data for the same incident energies in terms of the Feshbach-Kerman-Koonin (FKK) model for the preequilibrium process and the Hauser-Feshbach (HF) model for the equilibrium process. Using the same method of the FKK analysis as in Ref. (1), we have extracted the strength V_0 of the effective N-N interaction which is only a free parameter in the multi-step direct calculation. We discuss the incident energy dependence of the extracted V_0 values and the difference in them between (p,p') and (n,n') being pointed out in Refs. (1) and (2). In addition, we have found that isospin conservation plays a crucial role in multistep compound and HF processes in (p,p') at low incident energies of our interest.

References:
(1) Y. Watanabe et al., Phys. Rev. C **51** (1995) 1891.
(2) P. Demetriou et al., J. Phys. **G 22** (1996) 629.

---

*Japan Atomic Energy Research Institute
** The University of Tokushima

V. Nagoya University

A. Department of Energy Engineering and Science

V-A-1 Uncertainties in fission-product decay-heat calculations

K. Oyamatsu, H. Ohta, T. Miyazono and K.Tasaka

A paper on this subject was published in Proc. the First Internet Symposium on Nuclear Data (JAERI-Conf 97-004, pp. 141-148 (1997)) with the following abstract.

The present precision of the aggregate decay heat calculations is studied quantitatively for 50 fissioning systems. In this evaluation, nuclear data and their uncertainty data are taken from ENDF/B-VI nuclear data library and those which are not available in this library are supplemented by a theoretical consideration. An approximate method is proposed to simplify the evaluation of the uncertainties in the aggregate decay heat calculations so that we can point out easily nuclei which cause large uncertainties in the calculated decay heat values. In this paper, we attempt to clarify the justification of the approximation which was not very clear at the early stage of the study. We find that the aggregate decay heat uncertainties for minor actinides such as Am and Cm isotopes are 3-5 times as large as those for ^{235}U and ^{239}Pu. The recommended values by Atomic Energy Society of Japan (AESJ) were given for 3 major fissioning systems, ^{235}U(t), ^{239}Pu(t) and ^{238}U(f). The present results are consistent with the AESJ values for these systems although the two evaluations used different nuclear data libraries and approximations. Therefore, the present results can also be considered to supplement the uncertainty values for the remaining 17 fissioning systems in JNDC2, which were not treated in the AESJ evaluation. Furthermore, we attempt to list nuclear data which cause large uncertainties in decay heat calculations for the future revision of decay and yield data libraries.

V-A-2
Comparision of decay and yield data between JNDC2 and ENDF/B-VI

K. Oyamatsu, M. Sagisaka and T. Miyazono

A paper on this subject was published in Proc. the First Internet Symposium on Nuclear Data (JAERI-Conf 97-004, pp. 234-246 (1997)) with the following abstract.

This work is intended to be our first step to solve disagreements of the decay heat powers between measurements and summation calculations. We examine differences between nuclear data libraries to complement our uncertainty evaluation of the decay heat summation calculations only with ENDF/B-VI. The comparison is made mainly between JNDC2 and ENDF/B-VI while JEF2.2 decay data is also discussed. In this study, we propose and use a simple method which is an analogue of the overlap integral of two wave functions in quantum mechanics. As the first step, we compare the whole input nuclear data for the summation calculations as a whole. We find a slight difference of the fission yields especially for high-energy neutron induced fissions between JNDC2 and ENDF/B-VI. As for the decay energies, JNDC2, ENDF/B-VI are quite similar while JEF2.2 is found significantly different from these two libraries. We find substantial differences in the decay constant values among the three libraries. As the second step, we calculate the decay heat powers with FPGS90 using JNDC2 and ENDF/B-VI. The total decay heat powers with the two libraries differ by more than 10% at short cooling times while they agree well on the average at cooling times longer that 100 (s). We also point out nuclides whose contributions are significantly different between the two libraries even though the total decay heats agree well. These nuclides may cause some problems in predicting aggregate spectra of β and γ rays as well as delayed neutrons, and are to be reviewed in the future revision of decay and yield data.

V-A-3

Delayed Neutron Spectra and their Uncertainties in Fission Product Summation Calculations

T. Miyazono, M. Sagisaka, H. Ohta, K. Oyamatsu and M. Tamaki

A paper on this subject was published in Proc. the 1996 Nuclear Data Symposium (JAERI-Conf 97-005, pp. 83-88 (1997)) with the following abstract.

Uncertainties in delayed neutron summation calculations are evaluated with ENDF/B-VI for 50 fissioning systems. As the first step, uncertainty calculations are performed for the aggregate delayed neutron activity with the same approximate method as proposed previously for the decay heat uncertainty analyses. Typical uncertainty values are about 6~14% for 238U(F) and about 13~23% for 243Am(F) at cooling times 0.1~100 (s). These values are typically 2~3 times larger than those in decay heat at the same cooling times. For aggregate delayed neutron spectra, the uncertainties would be larger than those for the delayed neutron activity because much more information about the nuclear structure is still necessary.

V-A-4 Comparison of Yield and Decay Data among JNDC2, ENDF/B-VI and JEF2.2

K. Oyamatsu, M. Sagisaka and T. Miyazono

A paper on this subject was published in Proc. the 1996 Nuclear Data Symposium (JAERI-Conf 97-005, pp. 153-158 (1997)) with the following abstract.

Fission yields and decay data for fission product summation calculations are compared among JNDC2 and ENDF/B-VI and JEF2.2. Special attention is paid to the summation calculation of the total delayed neutrons per fission because it requires the data of the most unstable nuclides among all fission products. The cumulative fission yields of delayed neutron precursors are found to be appreciably different among the libraries even though values of the independent fission yields and the total number of delayed neutrons are chosen to be in fair agreement with each other. This suggests that there still exist large uncertainties in delayed neutron emission probabilities (or decay chains) for the precursors far from the stability line.

V-A-5

UNCERTAINTIES IN SUMMATION CALCULATIONS OF AGGREGATE DECAY HEAT AND DELAYED NEUTRON EMISSION WITH ENDF/B-VI

K.Oyamatsu, H.Ohta, T.Miyazono and M.Sagisaka

A paper on this subject will be published in Proc. Int. Conf. on Nuclear Data for Science and Engineering, May 1997, Trieste, Italy, with the following abstract.

Uncertainties in aggregate decay heat and delayed neutron activity calculations are evaluated for 50 fissioning systems with ENDF/B-VI. A simplification is made in the analyses in order to identify sources of the large uncertainties easily.

V-A-6

TWO METHODS FOR EVALUATION AND BENCHMARK TEST OF FISSION PRODUCT SUMMATION CALCULATIONS

K. Oyamatsu, M. Sagisaka, H. Takeuchi and T. Miyazono

A paper on this subject will be published in Proc. Int. Conf. on Nuclear Data for Science and Engineering, May 1997, Trieste, Italy, with the following abstract.

Fission yields and decay data for fission product summation calculations are compared among JNDC2 and ENDF/B-VI and JEF2.2. Special attention is paid to the summation calculation of the total delayed neutrons per fission because it requires the data of the most unstable nuclides among all fission products. The cumulative fission yields of delayed neutron precursors are found to be appreciably different among the libraries even though values of the independent fission yields and the total number of delayed neutrons are chosen to be in fair agreement with each other. This suggests that there still exist large uncertainties in delayed neutron emission probabilities (or decay chains) for the precursors far from the stability line.

V-A-7 Measurement of (n, α)cross sections for short-lived products by 13.4 - 14.9 MeV neutrons

Y. Kasugai[1], H. Yamamoto, K. Kawade and T. Iida[2]

A paper on this subject was submitted to Ann. Nucl. Energy in 1997.

Twelve (n, α) activation cross sections leading to short-lived nuclei with half-lives between 37 s and 15 min were measured in the energy range between 13.4 and 14.9 MeV by activation method. The measured reactions involved the isotopes of ^{26}Mg, ^{31}P, ^{54}Cr, ^{63}Cu, ^{64}Ni, ^{69}Ga, ^{71}Ga, ^{87}Ru, ^{89}Y, ^{104}Ru and ^{112}Cd. The intense 14 MeV neutron source facility (OKTAVIAN) at Osaka university was used for irradiation. The γ -rays emitted from the irradiated samples were measured with high-purity germanium (HPGe) detectors. All cross section values were obtained relative to the standard reaction cross section of ^{27}Al (n, α)^{24}Na. The cross sections of 4 reactions were measured for the first time. The present experimental data were discussed by comparing with previously reported experimental data and the evaluated data of JENDL-3 and ENDF/B-VI. The 6 evaluated data in JENDL-3 shows reasonable agreement within 7%, but the evaluation of ^{26}Mg reaction is 25% higher than our data. The 2 evaluation data of ENDF/B-VI agree well, but one evaluation is deviated more than 25% have been seen for 3 reactions.

---

[1]Present address; Japan Atomic Energy Research Institute.
[2] Department of electronic, information systems and energy engineering, Osaka University

V-A-8

Systematics for (n, α) excitations in the neutron energy between 13.3 and 15.0 MeV

Y. Kasugai[1], Y. Ikeda*, H. Yamamoto and K. Kawade

A paper on this subject was submitted to Ann. Nucl. Energy in 1997.

Systematics of (n, α) excitation functions in the neutron energy between 13.3 and 15.0 MeV were studied on the basis of experimental data measured by the Nagoya University and FNS groups (Japan Atomic Energy Research Institute). The empirical formulae of cross sections at 14.0 MeV (σ_{14}) and relative slopes of excitation functions (S) were deduced. These formulae covered the mass range between 19 and 188. The empirical formula of relative slope was expressed as a function effective threshold energy $E_{th} + V_\alpha$, where E_{th} is threshold energy and V_α is Coulomb barrier for α -particle emitted from the compound nucleus. The empirical formula of σ_{14} was expressed by a simple formula with two fitting parameters. By using the proposed empirical formulae, the partial excitation functions between 13 and 15 MeV were reproduced. Comparing the experimental data with the calculated excitations, we concluded that the accuracy of the proposed empirical formulae was ±30%.

---

[1]Present adress; Japan Atomic Energy Research Institute
*Japan Atomic Energy Research Institute

V-A-9 Measurement of (n,p)cross sections for short-lived products by 13.4 - 14.9 MeV neutrons

Y. Kasugai[1], H. Yamamoto, K. Kawade and T. Iida[2]

A paper on this subject was submitted to Ann. Nucl. Energy in 1997.

The 28 (n,p) activation cross sections leading to short-lived nuclei with half-lives between 20 s and 18 min were measured in the energy range between 13.4 and 14.9 MeV by activation method. The measured isotopes were ^{19}F, $^{28,29}Si$, ^{37}Cl, ^{50}Ti, $^{52,53,54}Cr$, $^{60,62}Ni$, $^{66,68}Zn$, $^{86,88}Sr$, ^{97}Mo, $^{101,102,104}Ru$, $^{104,105,108}Pd$, ^{107}Ag, ^{116}Cd and $^{119,120}Sn$ The intense 14 MeV neutron source facility (OKTAVIAN) at Osaka university was used for irradiation. The γ -rays emitted from the irradiated samples were measured with high-purity germanium (HPGe) detectors. All cross section values were obtained relative to the standard reaction cross section of ^{27}Al (n, α)^{24}Na. The present results were compared with previous data and the evaluated data of JENDL-3 and ENDF/B-VI. Ten reactions have been obtained at multi-point-energies for the first time. By using intense neutron sources and making careful corrections, reliable results could be obtained. Most of previous data obtained at multi-point-energies have shown reasonable agreement within 25%. In comparison of experimental 10 reactions with the evaluated data, significant discrepancies more than 25% have been seen for 3 reactions.

---

[1]Present address; Japan Atomic Energy Research Institute.

[2] Department of electronic, information systems and energy engineering, Osaka University

V-A-10 Measurement of Q_{EC}-value of ^{126}La isomers

Y. Kojima, M. Asai, A. Osa[1], M. Koizumi[1], T. Sekine[1],
M. Shibata, H. Yamamoto and K. Kawade,

A paper on this subject was submitted to Applied Radiation Isotopes in 1997

Beta-ray endpoint energies of the neutron-deficient nuclide of ^{126}La have been measured with an HPGe detector. The ^{126}La activities were produced by the ^{94}Mo (^{36}Ar, 3pn) reaction and mass-separated on-line. From the β - γ coincidence measurements, Q_{EC}-values of the high- and low- spin isomers of ^{126}La were determined for the first time to be 7700(100) keV and 7910(400) keV, respectively. The experimental atomic masses were compared with predicted values of mass formulas.

---

[1]Japan Atomic Energy Research Institute

V-A-11 Energy systematics of low-lying 0+ states in neutron-deficient Ba nuclei

M. Asai, T. Sekine[1], A. Osa[1], M. Koizumi[1], Y. Kojima,
M. Shibata, H. Yamamoto and K. Kawade

A paper on this subject was submitted to Phys. Rev. C in 1997

Low-spin states in ^{124,126,128,130}Ba fed by the EC/β^+ decay of their La parents have been investigated by means of γ - γ angular correlation measurement coupled with an isotope separator on-line. The spin of the first excited 0^+ states (0^+_2) were unambiguously established, and higher-excited 0^+ states were newly identified. The energy of the 0^+_2 state in ^{124}Ba previously assigned was revised upward. Resultingly, the level energy of the 0^+_2 state in neutron-deficient Ba nuclei takes a minimum at N=72 and then gradually increases toward neutron midshell (N=66), while the level energy of the 0^+_3 state rapidly decreases with decreasing neutron number. Their systematic behavior strongly suggests that the energy relation between the 0^+_2 and 0^+_3 state would invert at ^{122}Ba or at more deformed Ba nuclei, which is interpreted as the evolution of the 0^+_2 state in axially-symmetric deformed nuclei, while the 0^+_3 state toward the β-vibrational 0^+ state

[1]Japan Atomic Energy Research Institute

VI. Osaka University

A. Department of Nuclear Engineering

VI-A-1

Measurements of Double Differential Cross Sections of $^{51}V(n,xp)$, $^{51}V(n,x\alpha)$ and $^{nat}Zr(n,xp)$ Reactions by 14.1 MeV Incident Neutrons

Akito TAKAHASHI, Kokooo, Hiroyuki TAKAGI and Isao MURATA

The two dimensional E-TOF charged particle spectrometer has been developed and used to measure the double differential cross sections of charged particle emission reaction for several structural elements of fusion power reactor at OKTAVIAN, the Intense 14 MeV Neutron Source Facility of Osaka University.[1] [2] In 1997, we have done the experiment to measure DDX data for V(n,xp), V(n,xα) and Zr(n,xp) reactions. The measurements for vanadium were done also in 1996 but the the data were available up to 8 MeV. So, we have done the vanadium measurement again in 1997 to get a better data. The Li_2ZrO_3 has a potential to use as a breeding material in fusion power reactor. However, the DDX data of the proton emission reaction of natural zirconium is not available until now. So, we have done the measurement for $^{nat}Zr(n,xp)$ and compared with the evaluated nuclear data of JENDL Fusion File. The measured data for V(n,xp) reaction are good agreement with other experimental data, evaluated nuclear data of JENDL Fusion File and SINCROS-II calculation. In the case of $^{51}V(n,x\alpha)$ reaction, the measured EDX data is good agreement with SINCROS II calculation, while the JENDL-Fusion File shows good agreement with Grimes' data[3]. The total cross sections for vanadium measurement can be seen in Table.(1). The measured data and the evaluation for Zr show good agreement with each other as shown in Fig. 2.

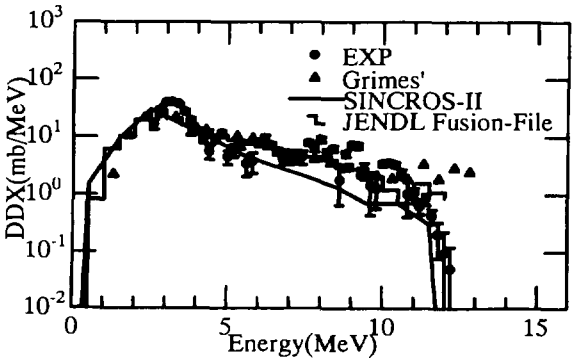

Fig. 1. EDX data of V(n,xp) reaction

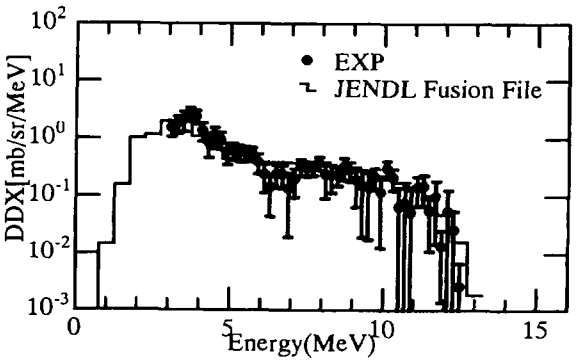

Fig. 2.The DDX data of Zr(n,xp) reaction at 45degree

	V(n,xp) mb	V(n,xα) mb
Present Work	84.25 ±1.61	16.71 ±2.312
Grimes	91±14	17±3
JENDL Fusion-file	85.4446	15.6003

Table. 1.Total cross- sections for vanadium

References:

(1)A. Takahashi, et al., Nucl. Instr. Meth A 401, 93 (1997).

(2)Kokooo, et.al.,"Measurements of double differential cross sections of charged particle emission reactions by 14.1 MeV incident neutrons", Proc. International Conference on Nuclear Data for Science and Technology, May. 19-24, 1997, Trieste, Italy, to be published.

(3)S.M Grimes, et al., Phys. Rev., C17, 508(1978).

VI-A-2

Benchmark Experiment on V, V-alloy, Li_2ZrO_3 and Li_2TiO_3 Assemblies with D-T Neutrons -Leakage Neutron Spectrum Measurement-

A.Takahashi, Kokooo, I.Murata, D.Nakano, F.Maekawa* and Y.Ikeda*

The benchmark experiments have been done for V, V-alloy(96%V, 4%Cr, 4%Ti), Li_2ZrO_3 and Li_2TiO_3 at two angle points, 0 degree and 24.9 degree by using slab assembly and time-of-flight (TOF) method[1] at Fusion Neutronics Source (FNS) in JAERI under the IEA collaboration. The efficiencies were determined by using SCINFUL calculation as well as the measured neutron spectra from beryllium assembly, graphite assembly, ^{252}Cf source and polyethylene. The data were obtained as low as 50 keV to perform the precise comparison with the evaluated nuclear data. The measured data were compared with MCNP-4A calculations which have been done by using evaluated nuclear data of JENDL-3.2, JENDL-Fusion File and FENDL/E-1.0. The measured data are almost good agreement with the evaluated nuclear data. The measured neutron angular flux spectrum compared with the evaluation for vanadium assembly of 15 cm thickness at 24.9 degree angle point is shown in Fig. 1.

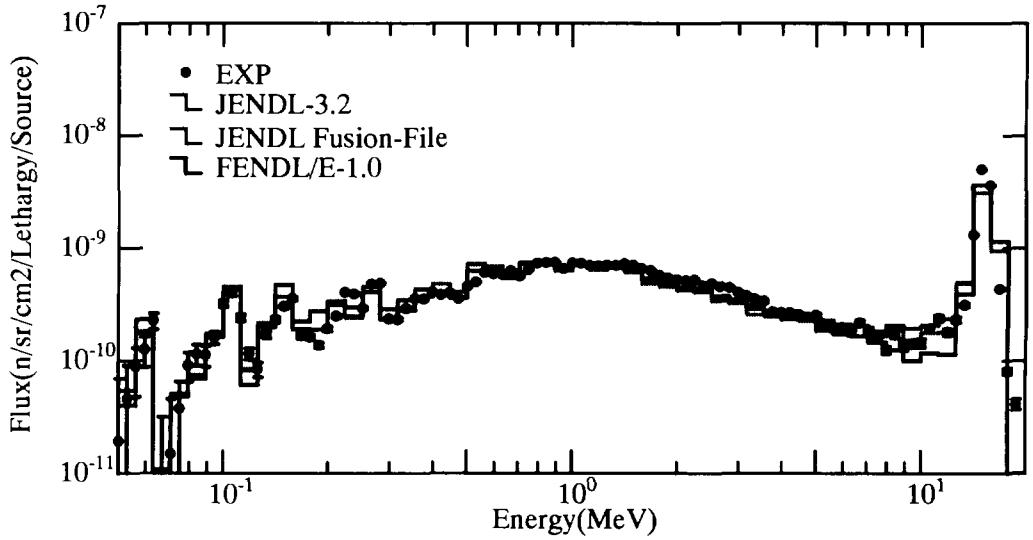

Fig. 1. The neutron flux spectrum at 25 degree for vanadium asembly of 15 cm thickness

Reference:

(1)Y. Oyama, H. Maekawa, Nucl. Instrum. Meth.,A245, 173

* High Energy Neutron Laboratory, Japan Atomic Energy Research Institute.

VI-A-3

Measurement of Reaction Cross Sections of Fission Products Induced by D-T Neutrons

Isao Murata, Daisuke Nakano and Akito Takahashi

The incineration of nuclear wastes, namely, minor actinides and fission products, has been widely investigated. With the view of future application of fusion reactor to incineration of fission products, we measured the $^{129}I(n,2n)^{128}I$ reaction cross section by D-T neutrons with the activation method.

The measurement was carried out using a continuous D-T neutron source of OKTAVIAN facility of Osaka University, Japan. The sample was a sealed source of ^{129}I, which was set up on the front surface of the water cooled fixed tritium target assembly and in the end section of a pneumatic tube of the irradiation and sample transport system. The effective reaction energy and neutron flux were determined by using Nb and Zr foils. The irradiating, cooling and counting periods were 60, 5 and 75 minutes in each run. After retrieving the sample by the pneumatic sample transport system, the gamma-rays from the irradiated sample were measured with a Hp-Ge detector.

The measured cross sections of $^{129}I(n,2n)^{128}I$ reaction in the neutron energies of 13.6, 14.2 and 14.6 MeV were 1.53 ± 0.20, 1.61 ± 0.21 and $1,58\pm0.21$ barn, respectively. In the determination of cross sections, a recently measured emission probability for the 443 keV gamma-ray emitted by the β^- decay of ^{128}I was referred as 0.12613 ± 0.00077 in Ref. (1). The evaluation of JENDL-3.2 underestimates the cross sections by about 9 % to the experimental result.

However, if emission probability is quoted from Table of Isotope[2], the measured cross sections are 1.14 ± 0.15, 1.20 ± 0.16 and 1.18 ± 0.16 barn, respectively, as described else where[3]. In this case, JENDL-3.2 overestimates the cross sections by about 25 %.

Reference:
(1) H. Miyahara, et al., Nucl. Instr. and Meth. in Phys. Res. A 353 (1994) 229.
(2) Table of Isotopes, Eighth Edition, John Wiley & Sons, Inc. (1996).
(3) D. Nakano et al., Proc. of the 1997 Symposium on Nuclear Data, JAERI, Tokai, Nov.27~28, 1997, to be published.

VI-A-4

Measurement of Nuclear Reaction Cross Sections of ^{9}Be induced by Low Energy Deuteron

A.Takahashi, K.Ochiai, K. Ishii, H. Miyamaru

Recently, beryllium (^{9}Be) metal and materials compounded ^{9}Be are prospective candidates for the first wall materials in of future fusion reactor. So we have measured the nuclear reaction cross sections of ^{9}Be induced by low energy deuteron.

This work has been done using OKTAVIAN at Osaka University and the tandem Pelletron 5SDH-2 at Kobe University of Mercantile Marine. A thick ^{9}Be metal foil (100μm) on an aluminum backing metal was used as the target. Charged particles emitted by ^{9}Be(d,x) reactions have been measured with a Si-Surface Barrier Detector (SSBD) set up at θ_{lab} =90°. Also, aluminum thin foil was set up in front of the SSBD for the screening of scattering deuteron and separation of the charge particles spectrum. As a result of the experiment, cross section of ^{9}Be(d,p)^{10}Be below 1000keV was obtained, e.g., 0.6-1.6μbarn/sr between 180 and 250keV. The energy dependent ^{9}Be(d,p)^{10}Be reaction cross section was reduced considering bare coulomb barrier transmission coefficient. Since the cross section might be enhanced by electron screening effect in ^{9}Be metal especially in lower energy region, We would try to measure the cross section in such a energy region aiming at investigation for very low energy nuclear reaction theory.

Reference:
(1) J.A.Biggerstaff, R.F.Hood, H.Scott and M.T.McEllistrem, Nucl.Phys. 36(1962)
(2) C.Rolf, Somorjai, Nucl. Instr. and Meth. B 99 (1995) 297-300

B. Department of Chemistry

VI-B-1

Specific Fission J-Window and Angular Momentum Dependence of the Fission Barrier

Hiroshi Baba*, Atushi Shinohara†, Tadashi Saito*, Naruto Takahashi*
and Akihiko Yokoyama*

A paper on this subject was published in Journal of the Physical Society of Japan, Vol. 66, No. 4 (1997) pp. 998-1009 with the following abstract.

Abstract:

A method to determine a unique J-window in the fission process was devised and the fissioning nuclide associated with thus extracted J-window was identified for each of the heavy-ion reaction systems. Obtained fission barriers at the resulting J-window were compared with the calculated values by the rotating finite range model (RFRM). The deduced barrier for individual nuclides were compared with the RFRM barriers to reproduce more or less the angular momentum dependence the RFRM prediction. The deduced systematic behavior of the fission barrier indicates no even-odd and shell corrections are necessary. The nuclear dissipation effect based on Kramer's model revealed substantial reduction of the statistically deduced barrier heights and brought a fairly large scattering from the RFRM J-dependence. However, introduction of the temperature-dependent friction coefficient ($\gamma = 2$ for $T \geq 1.0$ MeV and 0.5 for $T < 1.0$) was found to bring about satisfactory agreement with both RFRM fission barriers and the pre-fission neutron multiplicity systematics.

*Department of Chemistry, Graduate School of Science, Osaka University

†Department of Chemistry, Faculty of Science, Nagoya University

VI-B-2

Role of Effective Distance in the Fission Mechanism Study by the Double-Energy Measurement for Uranium Isotopes

Hiroshi Baba[‡], Tadashi Saito[‡], Naruto Takahashi[‡], Akihiko Yokoyama[‡],
Takahiro Miyauchi[‡], Sigehisa Mori[‡], Daisaku Yano[‡],
and Yoshihiro Nakagome[§]

A paper on this subject was published in Journal of Nuclear Science and Technology, Vol. 34, No. 9 (1997) pp. 871-881 with the following abstract.

Abstract:

Fission product kinetic energies were measured by the double-energy method for thermal-neutron fission of ^{235,233}U and proton-induced fission of ^{238}U at the 15.8-MeV excitation. From the obtained energy-mass correlation data, the kinetic-energy distribution was constructed from each mass bin to evaluate the first moment of the kinetic energy for a given fragment mass. The resulting kinetic energy was then converted to the effective distance between the charge centers at the moment of scission. The effective distances deduced for the proton-induced fission was concluded to be classified into two constant values, one for asymmetric and the other for symmetric mode, irrespective of the mass though an additional component was further extracted in the asymmetric mass region. This indicates that the fission takes place via two well-defined saddles, followed by the random neck rupture. On the contrary, the effective distances obtained for thermal-neutron induced fission turned out to lie along the contour line at the same level as the equilibrium deformation in the two-dimensional potential map. This strongly suggests that it is essentially a barrier-penetrating type of fission rather than the over-barrier fission.

[‡]Department of Chemistry, Graduate School of Science, Osaka University

[§]Research Reactor Institute, Kyoto University

VI-B-3

Charge Degree of Freedom as a Sensitive Probe for Fission Mechanism

A. Yokoyama[¶], H. Baba[¶], N. Takahashi[¶], M.-C. Duh[¶], and T. Saito[¶]

A paper on this subject was published in Journal of Radioanalytical and Nuclear Chemistry, Vol. 223, No. 1-2 (1997) pp. 99-120 with the following abstract.

Abstract:

The role of the charge degree of freedom in the heavy-ion-induced fission was investigated by carrying out a systematic analysis of radiochemically observed charge distribution in the fission of ^{238}U with ^{12}C ions of the incident energy between 85 and 140 MeV, particularly in connection with the energy given to the compound system. The charge distribution was found to follow essentially identical systematics as those which govern the light-ion fission except for the extremely weak energy dependence of the most probable charge Z_p. That is, values of the derivative of Z_p with respect to the energy were found quite small, or nearly zero, in the heavy-ion fission as compared with those of the light-ion fission. According to an analysis combining the derivatives of Z_p and fission neutron data, it was deduced that the excess energy given to the fused system was completely spent in the form of pre-scission neutrons and hence the number of post-scission neutrons remained constant as in the case of light-ion fission. The observed charge distribution was reproduced under the conditions that the relaxation of the charge degree of freedom be very fast and that the separation between the two potential fragments at the moment when the charge degree of freedom has been frozen is determined by using Viola's systematics on the fragment kinetic energy.

[¶]Department of Chemistry, Graduate School of Science, Osaka University

VII. Power Reactor and Nuclear Fuel Development Corp.

A. Nuclear Fuel Technology Development Division

VII-A-1 Measurement of Neutron Cross Section and Resonance Integral of the Reaction $^{133}Cs(n,\gamma)^{134}Cs$

Shoji Nakamura, Hideo Harada and Toshio Katoh

I. Introduction

More accurate neutron cross section data of long-lived fission product nuclides are of special importance for the transmutation study. In the case of the transmutation using reactor neutrons, particularly, the thermal neutron capture cross section (σ_0) and the resonance integral (I_0) are needed.

The present experiment was designed to measure more reliable data of the cross section and resonance integral for the formation of the isomeric state ^{134m}Cs and for the ground state ^{134g}Cs of the $^{133}Cs(n,\gamma)^{134}Cs$ reaction separately.

II. Experiment

The spec-pure (99.99%) cesium chloride powder was used as targets. The targets were prepared as following manner: First, cylindrical quartz cases (7mm in outer diameter, 1mm in thickness and 8mm in outer length) were weighed on a microbalance (Mettler model-UM3). About 12mg CsCl powder was poured into each weighing quartz case. They were housed in a oven and then heated at temperature up to 120°C for about 100 min in order to make CsCl powder anhydrous. After the end of heating, quartz cases were reweighed immediately on the microbalance. The amount of CsCl was determined quantitatively from the gain in weight of the quartz case. Finally, after weighing, each quartz case was sealed with a quartz plug and the ceramic bond whose principal component was aluminum oxide.

The irradiation of the target was performed with the Rikkyo Research Reactor at Rikkyo University, which reactor type is commonly known as TRIGA MK-II. Each target was housed in a polyethylene irradiation capsule, and placed in a rotary specimen rack (RSR), which was located in the reflector surrounding the reactor core. Some of targets were irradiated without a Cd shield capsule and others within a Cd shield capsule, which was 1mm in thickness, 22mm in outer diameter and 63mm in outer length. A Cd shield capsule was used in order to reduce the neutron flux at the irradiation position. In order to monitor the neutron flux, the wires of 0.112wt% Au/Al alloy (0.510 mm in diameter) and 0.46wt% Co/Al alloy (0.381mm in diameter) were used as activation detectors.

A high purity Ge detector was used to measure the γ-rays from the irradiated targets. Its performance was characterized as a 90 % relative efficiency to a 3" × 3" NaI(Tl) detector and 2.1 keV FWHM at 1.33MeV peak of ^{60}Co. The full energy peak efficiencies of the detector were calibrated with the standard γ-ray sources of ^{152}Eu and

^{133}Ba. The signals from the detector were fed to a fast data acquisition system, and then γ-ray spectra measured were recorded on a memory of a personal computer; the details of the data taking system were described elsewhere[1].

III. Result

Figure 1 shows the γ-ray spectra emitted from the Cs targets irradiated without and within a Cd shield capsule for 2 hours measurement, respectively. The γ-rays, originated from the isomeric state ^{134m}Cs and the ground state ^{134g}Cs induced by the ^{133}Cs(n,γ) reaction, were seen at the energies of 127, 563, 569, 605, 796 and 802keV. The γ-rays were used to estimate the activities, the half-lives and the reaction rates.

The half-life of the ^{134m}Cs was determined by following the decay of 127keV γ-ray intensity in order to identify the 127keV γ-ray peak as that of ^{134m}Cs. The resultant half-life was measured as 2.913 ± 0.003 hours. The present value was in good agreement with the evaluated value of 2.914 ± 0.003 (h)[2].

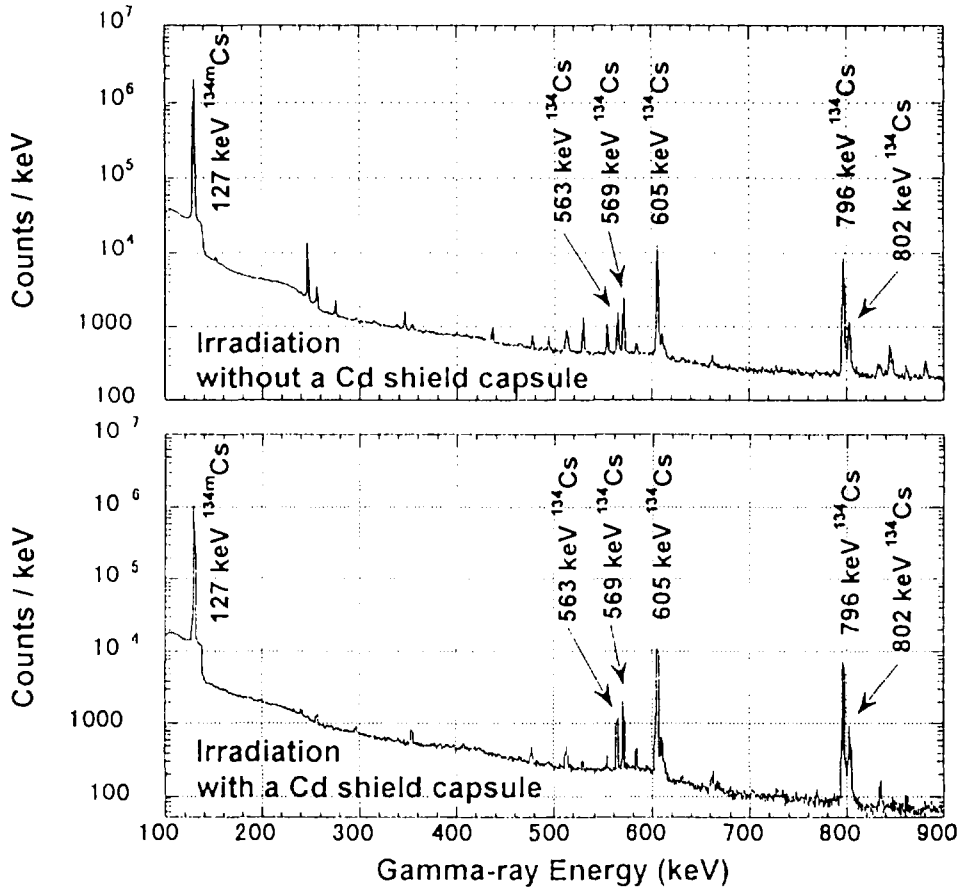

Fig. 1 Gamma-ray spectra of Cs targets irradiated without and within a Cd shield capsule by reactor neutrons

The analyses of the reaction rates of the ^{133}Cs targets and the flux monitors irradiated without and within a Cd shield capsule have given the thermal cross sections

and the resonance integrals for the $^{133}Cs(n,\gamma)^{134m,134g}Cs$ reaction as shown in **Table1**.

The thermal neutron capture cross section leading to the $^{134m+g}Cs$ agreed with the evaluated value and one leading to ^{134m}Cs was in good agreement with the data reported previously. The value of the isomer ratio estimated by the cross sections given in this work was in good agreement with the previous ones. On the other hand, the value of the resonance integral was 32% smaller than that reported by Steinnes et al[3].

Table 1 Results of neutron cross sections, resonance integrals and isomer ratio for the $^{133}Cs(n,\gamma)^{134m,134g}Cs$ reaction

	Present work		Previous measurements	
	σ_0 (barns)	I_0 (barns)	σ_0 (barns)	I_0 (barns)
to ^{134m}Cs	2.70 ± 0.15	23.2 ± 2.2	2.82 ± 0.07[4]	34.4 ± 1.9[4]
			2.44 ± 0.15[5]	
to ^{134g}Cs	26.3 ± 1.3	274 ± 23		
to $^{134m+g}Cs$	29.0 ± 1.3	297 ± 23	30.4 ± 0.8[4]	461 ± 25[4]
			29.0 ± 1.5[6]	437 ± 26[3]
			28.7 ± 0.7[7]	
isomer ratio	0.085 ± 0.006		0.085 ± 0.003[4]	
			0.086 ± 0.013[8]	

Acknowledgments

The authors wish to acknowledge their indeptedness to Prof. K. Tomura of Rikkyo University for his help and valuable discussions on the neutron irradiations and the activity measurements and to the crew of the Rikkyo Research Reactor for their cooperation.

This work was supported by PNC, and support by the Inter-University program for the Joint Use of Rikkyo University Reactor was also helpful and acknowledged.

References:

1) Harada, H., Nakamura, S., Ogata, Y., Katoh, T.: J. Nucl. Sci. Technol., **32**, 395 (1995).
2) Firestone, R.B., Shirley, V.S.: "*Table of Isotopes*", (8th ed.), John Wiley & Sons, Inc. New York (1996).
3) Steinnes, E.: J. Inorg. Nucl. Chem., **34**, 2699 (1972).
4) Baerg, A.P., Bartholomew, R.M.: Can. J. Chem., **38**, 2528 (1960).
5) Keisch, B.: J. Inorg. Nucl. Chem., **17**, 180 (1961).
6) Pomerance, H.: Phys. Rev., **83**, 641 (1951).
7) Takiue, M., Ishikawa, H.: Nucl. Instr. And Meth., **148**, 157 (1978).
8) Bishop, C.T., Vonach, H.K., Huizenga, J.R.: Nucl. Phys., **60**, 241 (1964).

VII-A-2

Measurement of Thermal Neutron Capture Cross Section and Resonance Integral of the Reaction $^{127}I(n,\gamma)^{128}I$

Toshio KATOH[1], Shoji NAKAMURA, Hideo HARADA
and Yoshimune OGATA[2]

1. Introduction

The measurement of the thermal neutron(2,200 m/s neutron) capture cross section(σ_0) and the resonance integral(I_0) of the reaction $^{127}I(n, \gamma)^{128}I$ were carried out along with the measurement of those of the reaction $^{129}I(n, \gamma)^{130}I$ by the activation method in order to obtain fundamental data for research on the transmutation of the nuclear wastes. The most of references published previously reported either of σ_0 or I_0. The purpose of the present experiment is to perform simultaneous measurement of the σ_0 and the I_0 of ^{127}I by using an activation method.

2. Experiment

The targets of the iodine including ^{127}I and ^{129}I were irradiated within and without a cadmium shield capsule in the Rotary Specimen Rack(RSR) of Rikkyo University Research Reactor. Two kinds of flux monitor wires, Co/Al and Au/Al wires, were irradiated at the same position as the iodine targets to monitor the thermal neutron flux and the fraction of the epithermal component(Westcott's index).

The yields of γ-rays emitted from the irradiated targets were measured using a high purity Ge detector with a 90% relative efficiency and an energy resolution of 2.1 keV FWHM at 1.33 MeV. Gamma-ray spectra obtained are shown in **Fig. 1.**

To correct the full energy peak efficiency for the pulse pile-up loss, the counting loss of pulse from a pulser was measured in advance as a function of the ratio of ADC live time to its real time. The correction factor of the pulse pile-up loss for the γ-rays detected was obtained by inserting the ratio of ADC live time to the real time for each measurement into this function.

---

1) Power Reactor and Nuclear Fuel Development Corp.
and Gifu College of Medical Technology
2) Radioisotope Research Center, Nagoya University

Gamma-ray spectra were taken successively and the decay of peak intensity of the 443 keV γ-ray of ^{128}I were followed. A half-life of ^{128}I obtained from the decay of the 443 keV γ-ray intensity was 24.72 ± 0.03 min.

The radioactivities of the flux monitor wires were measured with the same Ge detector. The thermal neutron flux at the irradiation position was 4.6 x 10^{11} n/(cm^2·s) and the epithermal index in the Westcott's convention was 0.038.

3. Result

In Fig. 1, γ-ray peaks from ^{128}I produced by the ^{127}I(n, γ)^{128}I reaction were observed at energies of 443, 527 and 969 keV. The intense γ-ray peak of ^{128}I at 443 keV was used for the determination of the reaction rate to generate the ^{128}I.

When an effective cross section $\hat{\sigma}$ for well moderated neutrons is expressed by the Westcott convention, the reaction rate R is given by the following equation,

$$R = nv_0\hat{\sigma}, \tag{1}$$

where nv_0 is the "neutron flux" in the Westcott convention with the neutron density n, including thermal and epithermal neutrons, and with the velocity of neutron v_0 = 2,200 m/s, and

$$\hat{\sigma} = \sigma_0 [gG_{th} + r(T/T_0)^{1/2} s_0 G_{epi}] . \tag{2}$$

Here, σ_0 is the reaction cross section for 2,200 m/s neutrons, and g the measure of the cross section deviation from the $1/v$ law in the thermal energy region. The quantity $r(T/T_0)^{1/2}$ gives the fraction of epithermal neutron in the neutron spectrum, and s_0 is defined by

$$s_0 = \frac{2}{\pi^{1/2}} \cdot \frac{I_0}{\sigma_0}, \tag{3}$$

with I_0, the resonance integral after subtracting the $1/v$ component. The G_{th} and G_{epi} denote self-shielding coefficients for thermal and epithermal neutrons, respectively. The value of gG_{th} was set to unity in the following analysis, since g and G_{th} are almost unity in this experiment. The value of G_{epi} was also set to unity.

Equation(1) with Eqs.(2) and (3) is written in simplified forms as

$$R/\sigma_0 = \phi_1 + \phi_2 s_0, \tag{4}$$

for irradiation without a Cd shield capsule, and

$$R'/\sigma_0 = \phi'_1 + \phi'_2 s_0, \tag{5}$$

for irradiation within a Cd shield capsule.

The values of simplified flux factors, $\phi_{1,2}$ and $\phi'_{1,2}$ were determined using the R and R' values of the flux monitor wires, Co/Al and Au/Al. The $\phi_{1,2}$ and $\phi'_{1,2}$

obtained are summarized in **Table 1.**

Since Eqs.(4) and (5) give a relation,

$$s_0 = -\frac{\phi_1 - \phi'_1\left(R/R'\right)}{\phi_2 - \phi'_2\left(R/R'\right)}, \qquad (6)$$

the s_0 value of the ^{127}I(n, γ)^{128}I reaction is deduced from the R/R' value of irradiated ^{127}I samples. The value of σ_0 is obtained by substituting the s_0 into Eq.(4). The value of I'_0 is then obtained using Eq.(3).

The resonance integral I_0 is calculated by assuming the Cd cut-off energy to be 0.55 eV, where the effective thickness of the Cd shield was estimated to be 1.4 mm by considering neutrons penetrating obliquely through the cylindrical Cd shield capsule of thickness of 1.0 mm. Then, the resonance integral I_0 is given by

$$I_0 = I'_0 + 0.429\sigma_0, \qquad (7)$$

where $0.429\sigma_0$ is the $1/v$ contribution.

The thermal neutron capture cross section(σ_0) and the values of s_0, I'_0 and I_0 obtained from the above analysis are shown in **Table 2.** Weighted average of the σ_0 and the I_0 of the reaction ^{127}I(n, γ)^{128}I obtained were 6.40 ± 0.34 barns and 162 ± 12 barns, respectively.

Table 1 Results of neutron flux measurements in Rotary Specimen Rack Rikkyo Reactor

Irradiation type	irradiation period	ϕ_1 or ϕ'_1 (10^{11} n/(cm^{2}s))	ϕ_2 or ϕ'_2 (10^{11} n/(cm^{2}s))
Without Cd	10 min	4.618 ± 0.098	0.173 ± 0.013
Within Cd	10 min	0.122 ± 0.012	0.178 ± 0.005

Table 2 Present results of measurement of σ_0 of I_0 of ^{127}I

	Run 1	Run 2	Run 3	Weighted average
σ_0 (barns)	6.37 ± 0.35	6.68 ± 0.36	6.09 ± 0.33	6.40 ± 0.34
s_0	28.7 ± 1.6	26.5 ± 1.5	29,5 ± 1.7	28.0 ± 1.5
I'_0(barns)	162 ± 13	157 ± 12	160 ± 12	159 ± 12
I_0(barns)	164 ± 13	160 ± 13	162 ± 13	162 ± 12

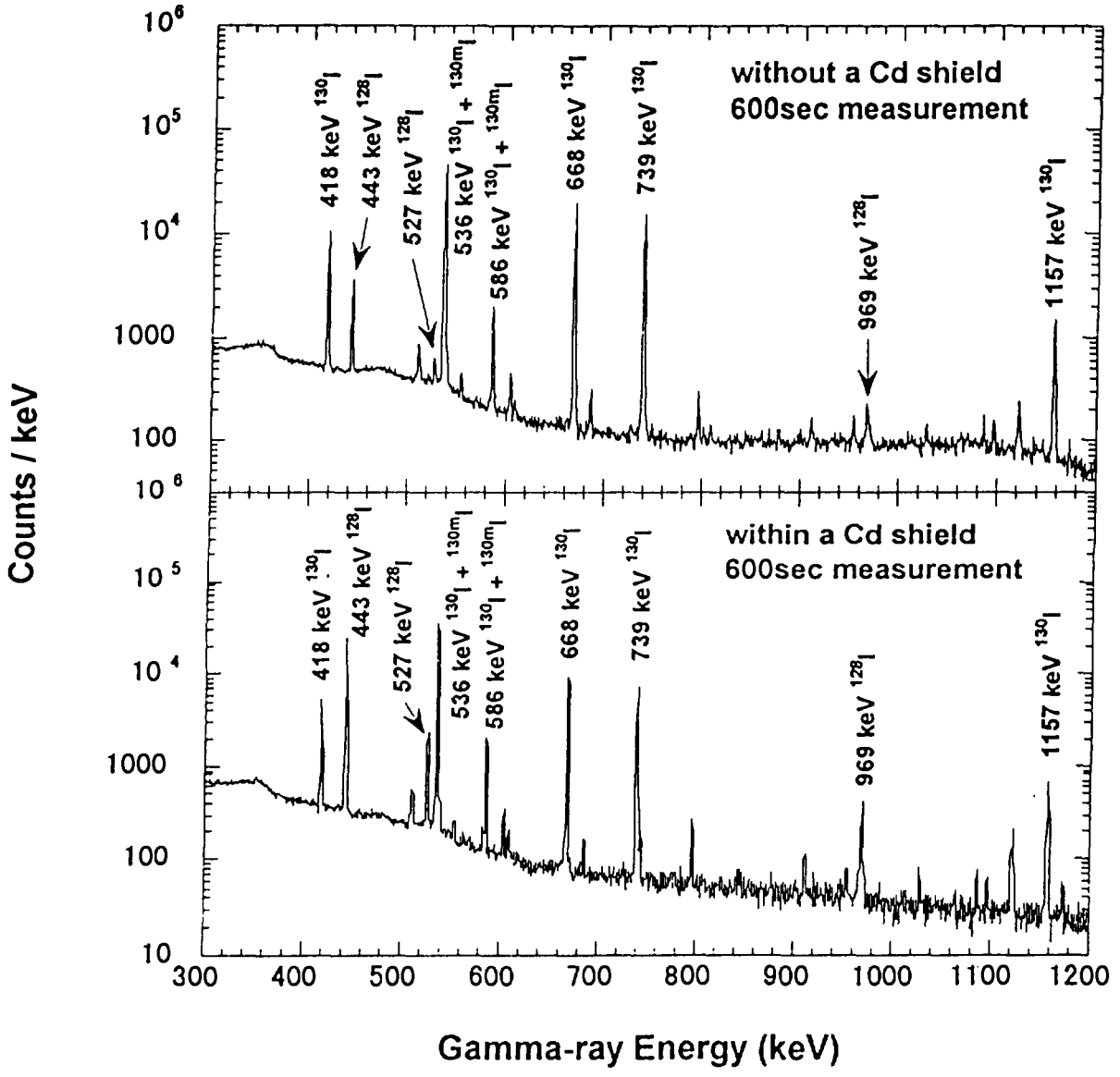

Fig. 1 . Gamma-ray spectra of ^{127}I-^{129}I targets irradiated without and within a Cd shield capsule

VII-A-3 Measurement of Thermal Neutron Cross Section and Resonance Integral of the Reaction $^{135}Cs(n, \gamma)^{136}Cs$

T. Katoh[1], S. Nakamura, H. Harada, Y. Hatsukawa[2], N. Shinohara[2], K. Hata[2], K. Kobayashi[2], S. Motojima[2], M. Tanase[2]

A paper on this subject was published in J. Nuclear Science and Technology vol. 34, no.5, pp431～438(1997) with a following abstract.

The thermal neutron(2,200 m/s neutron) capture cross section(σ_0) and the resonance integral(I_0) of the reaction $^{135}Cs(n, \gamma)^{136}Cs$ were measured by means of an activation method to obtain fundamental data for research on the transmutation of nuclear waste. Targets of radioactive cesium, which include ^{135}Cs and ^{137}Cs as well as stable ^{133}Cs, were irradiated with reactor neutrons within or without a Cd shield case. The Co/Al and Au/Al alloy wires as activation detectors were irradiated together with cesium samples to monitor the neutron flux and the fraction of the epithermal part(Westcott's index). A high purity Ge detector was used for the γ-ray measurements. The ^{137}Cs nuclide was used as a tracer of ^{135}Cs, since ^{135}Cs decays through a β-transition, but does not emit γ-rays. The ratio of the number of nuclei of ^{135}Cs to that of ^{137}Cs in the target was measured with a quadrupole mass spectrometer. This ratio and the ratio of activity of ^{136}Cs to that of ^{137}Cs in the irradiated target were used for deduction of the σ_0 and the I_0 of ^{135}Cs. The σ_0 and the I_0 of the reaction $^{135}Cs(n, \gamma)^{136}Cs$ were 8.3 $\pm$ 0.3 barn and 38.1 $\pm$ 2.6 barn, respectively. The σ_0 is in agreement with that reported by Baerg et al., while the I_0 is about 2/3 of that reported by Baerg et al.

---

1) Power Reactor and Nuclear Fuel Development Corp.
and Gifu College of Medical Technology
2) Japan Atomic Energy Research Institute

VIII. Tohoku University

A. Department of Quantum Science and Energy Engineering

VIII-A-1 Measurement of $^{14}N(n,p)^{14}C$ Cross Section for kT=25.3 keV Maxwellian Neutrons using a Gridded Ionization Chamber

Toshiya Sanami, Mamoru Baba*, Isamu Matsuyama, Sigeo Matsuyama
Takehide Kiyosumi, Yasushi Nauchi and Naohiro Hirakawa

A paper on this subject has been published in Nuclear Instruments and Methods A394 (1997) p.368-373 with the following abstract:

We measured the $^{14}N(n,p)^{14}C$ reaction cross section for neutrons with a quasi Maxwellian distribution of kT=25.3 keV which is one of the key parameters for the s-process nucleosynthesis in astrophysics. Protons were detected with high efficiency using a gridded ionization chamber. We employed a thick Li target and a 1.912 MeV proton beam for neutron production, and a vacuum-evaporated melamine ($C_3H_6N_6$) film as a ^{14}N sample. The absolute cross section was determined relatively to the $^6Li(n,t)\alpha$ cross section by measuring the triton yield from a ^6LiF film in place of melamine. Our result (1.70 ± 0.08 mb) is approximately a factor 2 larger than the value reported in an ealier direct measurement for the same Maxwellian neutron spectrum; it is consistent with results deduced from monoenergetic neutrons or inverse reaction.

VIII-A-2

Measurements of Double-differential Neutron Emission Cross Sections and Development of a Wide Range Charged Particle Spectrometer for ten's MeV Neutrons

Y.Nauchi, M.Baba, T.Kiyosumi, T.Iwasaki, T.Sanami, S.Matsuyama, N,Hirakawa
Su.Tanaka[a], S.Meigo[b], H.Nakashima[b], T.Nakamura[c]

A paper on this subject has been published in JAERI-Conf 97-005 (1997) p.126-131 with the following abstract:

We measured (n,xp), (n,xd) cross sections of C and Al for En=64.3 MeV neutrons at the ^{7}Li(p,n) neutron source facility at TIARA (Takasaki Establishment, JAERI) by using a conventional SSD-NaI telescope placed in the air. They show characteristic energy and angular dependence in high energy region.

In order to extend the measurements to low energy protons and α particles, a spectrometer consisting of low pressure gas counters and BaF_2 scintillators is now under development. A low threshold for low energy α particles will be achieved by using the gas counter. The particle identification over a wide energy range will be achieved by combining the ΔE-E method for low energy particles with the pulse shape discrimination (PSD) method of BaF_2 for high energy particles.

---

a: Takasaki Establishment, Japan Atomic Energy Research Institute
b: Tokai Establsihement, Japan Atomic Energy Research Institute
c: Cyclotron Radioisotope Center, Tohoku University

VIII-A-3

Measurements of Double-differential Neutron Emission Cross Sections of ^{6}Li and ^{7}Li For 18 MeV Neutrons

Masanobu Ibaraki, Mamoru Baba, Shigeo Matsuyama, Toshiya Sanami, Than Win, Takako Miura and Naohiro Hirakawa

A paper on the subject has been published in JAERI-Conf 97-005 (1997) p.164-168 with the following abstract:

Double-differential neutron emission cross sections of ^{6}Li and ^{7}Li were measured for 18 MeV neutrons at Tohoku University 4.5 MV Dynamitron facility. Neutron emission spectra were obtained down to 1 MeV at 13 angles with energy resolution good enough to separate discrete levels. A care was taken to eliminate the sample-dependent background due to parasitic neutrons. Experimental results were in fair agreement with the JENDL-3.2 data and a simple model considering a three-body breakup process and discrete level excitations.

VIII-A-4 (n, α) Cross Section Measurement of Gaseous Samples using Gridded Ionization Chamber - Cross Section Determination -

Toshiya Sanami, Mamoru Baba, Keiichiro Saito, Yasutaka Ibara and Naohiro Hirakawa

A paper on the subject has been published in JAERI-Conf 97-005 (1997) p.176-181 with the following abstract:

We are developing a method of (n, α) cross section measurement using gaseous samples in a gridded ionization chamber (GIC). This method enables cross section measurements in large solid angle without the distortion by the energy loss in a sample, but requires a method to estimate the detection efficiency. We solve the problem by using GIC signals and a tight neutron collimation. The validity of this method was confirmed through the $^{12}C(n, \alpha_0)^9Be$ measurement. We applied this method to the $^{16}O(n, \alpha)^{13}C$ cross section around 14.1 MeV.

B. Laboratory of Nuclear Science

VIII-B-1

Angular correlations for the $^{12}C(e,e'n)^{11}C$ reaction in the giant resonance region

T. Saito, S. Suzuki, K. Takahisa, C. Takakuwa, M. Oikawa,
T. Tohei* T. Nakagawa* and K. Abe†

A paper on this subject was published in Phys. Rev. Lett. 78, 1018 (1997) with the following abstract:

Angular correlations for the $^{12}C(e,e'n)^{12}C$ reaction in the giant resonance region have been measured for forward scattering at an effective momentum transfer of 0.35 fm^{-1}. The angular correlations for the ground-state transition indicates a strong forward-backward asymmetry at the peak of the giant dipole resonance (ω = 22.5 MeV) , which is different from the nearly symmetric angular correlations observed for the $^{12}C(e,e'p_0)^{11}B$ reaction. Recent RPA predictions fail to reproduce the experimental angular correlations for both ($e,e'n_0$) and ($e,e'p_0$), predicting the opposite patterns to those observed.

*Department of Physics, Tohoku University
†Department of Nuclear Engineering, Tohoku University

VIII-B-2 Study of the giant resonance of ^{16}O by the (e,e'n) reaction

K. Kouichi, T. Saito, Y. Suga[1], T. Endo, K. Yoshida, K. Takahashi, T. Nakagawa[2], K. Abe[3] and H. Ueno[4]

In study of the giant resonance, ^{16}O nucleus is one of the well studied nuclei. The cross section of the GDR in ^{16}O consists of the two major peaks corresponding to mainly $(1d_{5/2},1p_{3/2}^{-1})$, $(1d_{3/2},1p_{3/2}^{-1})$ 1p-1h configurations. In addition, $^{16}O(\alpha,\alpha'\alpha)$,$^{16}O(e,e'\alpha)$ and ^{15}N $(\vec{p},\gamma_0)$ experiments have revealed that the IS- and IV-GQR exist in the low and high GDR region respectively. In this report we introduce the result of the $^{16}O(e,e'n)$ angular distribution measurement. Angular distributions are sensitive to resonances and they reflect an existence of a weak resonance in a strong one through the effect of interference between these resonances. So we intend to see the isospin dependency of the interference effect between the GDR and the IS- or IV-GQR. An RPA calcuration[1)] with the SK3 effective interaction supports this expectation. It predicts that an $(e,e'n_0)$ angular distribution at low excitation energy shows a strong backward peak because of the interference between the GDR and the IS-GQR, but shows a strong forward peak at high excitation energy because of that between the GDR and the IV-GQR.

The $^{16}O(e,e'n)$ experiment has been done using a 129 MeV continuous electron beam. Scattered electrons were momentun analyzed with a double-focused spectrometer settled at θ_e=30° in the excitation energy range of 20~30MeV. It corresponds to a momentum transfer 0.33 fm^{-1}. Neutrons were detected by the 10 liquid scintillation counters surround the target at a distance of 1 meter. The neutron energy was decided by the TOF method. We used a natural target of Li_2O (100.6mg/cm^2, mainly ^{16}O and ^{7}Li).

Figure 1 shows a missing energy distribution. We can see n_0 and n_3 peaks. These two peaks show a 1p-1h coherency of the giant resonance, because the configurations of the residual nucleus ^{15}O corresponding to n_0 and n_3 decays are $1p_{1/2}^{-1}$ and $1p_{3/2}^{-1}$ of ^{16}O respectively. On the other hand for near another decay channels n_1,n_2 and n_4, the residual nucleus ^{15}O has even parity and its configuration is much more complex than that of n_0 or n_3.

Figure 2 shows $^{16}O(e,e'n_0)$ angular distributions. At the whole excitation energy we can see two peaks at q- and anti q-direction. This is the specific feature that the resonance is mainly E1. But the strengths of these peaks are not equal. It is due to the fact that E2 resonance exists at the same excitation enrgy. The forward peak at the low excitation energy is bigger than the backward one and this feature is much different

[1]Present Address: Hitachi Software.
[2]Department of Physics, Tohoku Univ.
[3]Department of Nuclear Engineering, Tohoku Univ.
[4]Department of Physics, Yamagata Univ.

from the prediction by the RPA calucuration. The angular distributions at the high excitation energy are same as lower ones. The RPA calcuration predicts a shape of the angular distribution well but does not reproduce the magnitude. Our results are similar to those of $^{16}O(e,e'p_0)$ experiment[2] in the whole excitation energy at a similar momentunm transfer. However it is difficult to discuss the isospin dependency of the interference in the (e,e'p) reaction since the contribution from a quasi-elastic process must be subtracted from the resonance.

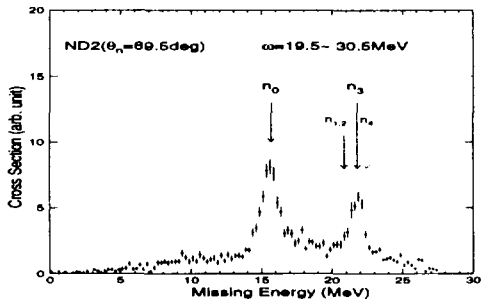

Fig. 1. $^{16}O(e,e'n)$ reaction missing energy distribution. The n_0 stands for the reaction that residual nucleus ^{15}O is the ground state and n_1, n_2, n_3 and n_4 stand for that ^{15}O is the excited state.

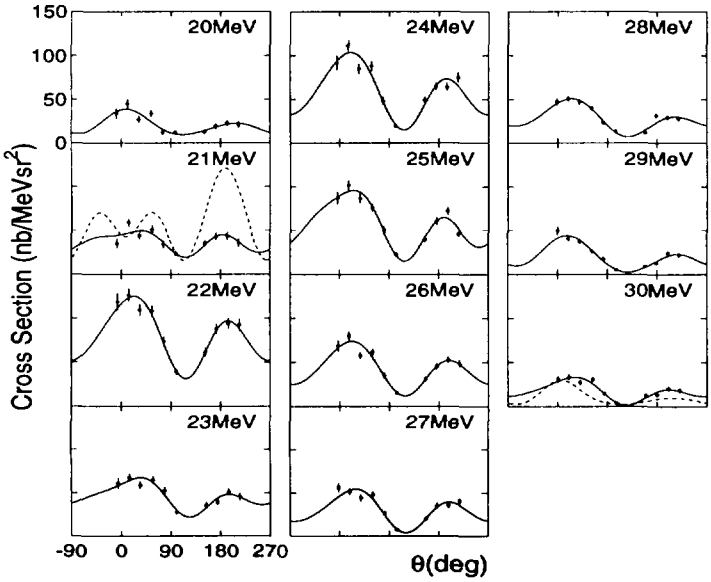

Fig. 2. $^{16}O(e,e'n_0)$ angular distribution. θ is the angle of the neutron emission with respect to the direction of the momentum transfer. Solid lines are the χ^2 fits by the Legendre polynomials. Dotted lines represent the RPA calculation[1] with the SK3 effective interaction. The calculations are normalised to the values of solid lines at θ=0°.

References:

1) M. Cavinato, M. Marangoni and A. M. Saruis : Phys.Lett. 163B (1985) 49.

2) V. F. Dmitriev, D. M. NIkolenko, S. G. Popov, I. A. Rachek and D. K. Toporkov : Nucl.Phys. A464 (1987) 237.

C. Cyclotron and Radioisotope Center

VIII-C-1 Neutron activation cross sections of ^{12}C, ^{27}Al, ^{59}Co, ^{nat}Cu, and ^{209}Bi nuclides in the energy range of 20MeV to 150MeV

E. Kim[1], T. Nakamura[1], Y. Uwamino[2], M. Imamura[3], N. Nakao[4], Su. Tanaka[5]

The neutron activation cross sections of ^{12}C, ^{27}Al, ^{59}Co, ^{nat}Cu and ^{209}Bi nuclides have been measured in the quasi-monoenergetic p-Li neutron fields in the energy range of 20MeV to 150MeV. The irradiation experiments were performed at four cyclotron facilities of 1) INS of Univ. of Tokyo, 2) CYRIC of Tohoku Univ., 3) TIARA of JAERI, and 4) RIKEN. Our experimental data were compared with other experimental and calculated data and the ENDF/B-VI high energy file data.

1. INTRODUCTION

With the increasing use of the high energy and high intensity accelerators, the radioactivities induced in the accelerator materials, shielding materials and the air and water of accelerator facility bombarded by the primary accelerating charged particles as well as the secondary neutrons have become a serious problem. Nevertheless, neutron activation cross section data in the energy range above 20MeV are very poor mainly due to very limited number of facilities having quasi-monoenergetic neutron fields. We measured the neutron activation cross sections of ^{12}C, ^{27}Al, ^{59}Co, ^{nat}Cu, and ^{209}Bi nuclides by using the quasi-monoenergetic p-Li neutron fields at four cyclotron facilities of 1) Institute for Nuclear Study (INS), University of Tokyo [1], 2) Cyclotron and Radioisotope Center (CYRIC), Tohoku University [1], 3) Takasaki Research Establishment (TIARA), Japan Atomic Energy Research Institute [2], and 4) Institute of Physical and Chemical Research (RIKEN) [3].

2. EXPERIMENT

The irradiation experiments were performed in the quasi-monoenergetic neutron fields produced by the $^{7}Li(p,n)$ reaction, which have been established at three cyclotron facilities of the AVF cyclotron at INS for 20 to 40MeV, of the AVF cyclotron at TIARA for 40 to 90MeV, and of the Separate-Sector (Ring) cyclotron at RIKEN for 80 to 150MeV. The Li-targets of 2 to 10 mm thicknesses were bombarded by proton beams of 20 to 150 MeV energies which were extracted from these cyclotrons. The neutrons produced in the forward direction from the target were transported through the collimator for sample irradiation and the proton beams passed through the target were swept out by the magnet to the beam dump at CYRIC, TIARA and RIKEN. The neutron spectra were measured with the TOF method using a NE213 liquid organic scintillator. The absolute neutron fluence was determined with the PRT(Proton Recoil counter Telescope) at TIARA, and with the Li activation method to detect the ^{7}Be activity from the $^{7}Li(p,n)^{7}Be$ reaction at CYRIC and RIKEN. The p-Li neutron field at INS has a small space and the neutron TOF measurement could not be done, then the neutron spectra measured at the CYRIC p-Li neutron field were used instead.

Table I summarizes the physical data of irradiation samples used at INS, TIARA and RIKEN. At INS, the samples were irradiated for 4 to 13 hours, and at TIARA and RIKEN the irradiation time consisted of short irradiation time (1 to 2 hours under 120MeV, 30min above 120MeV) and long irradiation time (about 20 hours) by considering the half lives of produced nuclei.

The proton beam current during irradiation was recorded by the digital current integrator, connected to a multi-channel scaler with the dwelling time of 10sec, 60sec and 60sec at INS, TIARA and RIKEN, respectively, to monitor fluctuations of the neutron fluence.

[1] Cyclotron and Radioisotope Center, Tohoku University
[2] Institute of Physical and Chemical Research
[3] National Museum of Japanese History
[4] High Energy Accelerator Research Organization
[5] Takasaki Research Establishment, Japan Atomic Energy Research Institute

After the irradiation, the gamma rays emitted by the irradiated samples were measured with a high purity HP-Ge detector. These samples were counted several times to identify the half-lives of the activities produced.

3. ANALYSIS

Estimation of photo-peak area of gamma-ray spectra which were measured by the HP-Ge detector was done with the computer program for the automatic analysis of gamma-ray spectrum by Komura et al [4] or the direct counting of eye-fitting peak area only for very weak photo-peaks.

The reaction rates of radioisotopes identified from the gamma-ray spectra and the decay curves were estimated after corrected for the peak efficiency of Ge detector, the coincidence-summing effect, self-absorption effect in thick samples, and also for the beam current fluctuation during sample irradiation. The peak efficiency of the HP-Ge detector was determined by using the standard mixed gamma-ray source and the correction factor for self absorption of gamma rays in the samples was calculated by the Monte Carlo code, PEAK [5] for the INS and TIARA experiments, but for the RIKEN experiment, the peak efficiencies of the HP-Ge detector including the self-absorption of the irradiated samples were calculated simultaneously by the electron-photon cascade Monte Calro code, EGS4[6], due to very thick samples as seen in Table I. The coincidence-summing effect caused by the coincidence detection of two or more gamma rays in the gamma ray spectrum was corrected by using the SUMECC code [7].

The obtained reaction rate is connected to neutron cross section σ(E) as follows,

$$R = \int_{Eth}^{E_{max}} \sigma(E) \cdot \phi(E) \cdot dE \,, \qquad (1)$$

where $\phi(E)$ is the neutron fluence ($n \cdot cm^{-2} \cdot MeV^{-1} \cdot Coulomb^{-1}$), E_{th} the threshold energy and E_{max} the maximum energy of the monoenergetic peak neutrons.

The cross section at the effective energy of peak neutrons $\sigma(E_{eff})$ can be obtained, after corrected the contribution of low-energy tail neutrons to the obtained reaction rate as follows

$$\sigma(E_{eff}) = \frac{R \cdot f}{\phi(E_{peak})} \,. \qquad (2)$$

The f value is the ratio of peak reaction rate from E_{min} (minimum energy of the monoenergy peak) to E_{max} and total reaction rate from E_{th} to E_{max}, the peak-to-total ratio of reaction rate, which is expressed as,

$$f = \frac{\int_{E_{min}}^{E_{max}} \sigma(E) \cdot \phi(E) \cdot dE}{\int_{E_{th}}^{E_{max}} \sigma(E) \cdot \phi(E) \cdot dE} \,. \qquad (3)$$

The f value is at first estimated from the lowest peak neutron energy by using the measured neutron flux, $\phi(E)$ and the cross section, $\sigma(E)$, of the evaluated high energy data files, ENDF/B-VI[8] or experimental data complied by McLane et al.[9] . By using thus-obtained f value, the cross section at the higher peak neutron energy, $\sigma(E_{eff})$ can be calculated from Eq.(2).

The statistical errors of the reaction rates were about 0.5% to 11% depending on the gamma-ray peak counts of irradiated samples. The errors of peak neutron fluences were between 12% and 14%. The error of the f value which was used for the correction of the contribution to the reaction rate due to the low-energy neutron tail was estimated to be 2% to 35% at maximum by combining the neutron flux error of 2% to 7% with the cross section error between 1% and 35% according to the variations observed for the published data.

4. RESULTS AND DISCUSSION

The neutron activation cross sections of 20 reactions occured in ^{12}C, ^{27}Al, ^{59}Co, ^{nat}Cu, and ^{209}Bi nuclides were measured in the energy range of 20 to 150MeV. As examples, Figs. 1 to

6 give the cross section data of $^{12}C(n,2n)$, $^{27}Al(n,2n\alpha)^{22}Na$, $^{59}Co(n,3n)^{57}Co$, $^{nat}Cu(n,sp)^{58}Co$ and $^{209}Bi(n,xn)^{210-x}Bi$ reactions, respectively, compared with other experimental data and ENDF/B-VI high energy file data. We found that the measured $^{12}C(n,2n)^{11}C$ cross section has a constant value of about 20mbarn in the energy range above 40MeV differently from the ENDF/B-VI data. The experimental cross section data of $^{59}Co(n,3n)^{57}Co$ show good agreement with the calculation data by Odano[10]. The obtained data of $^{27}Al(n,2n\alpha)^{22}Na$, $^{nat}Cu(n,sp)^{58}Co$ and $^{209}Bi(n,xn)^{210-x}Bi$ were compared with the ENDF/B-VI high energy file data calculated with the ALICE code[11] by Fakahori. Our experimental results for ^{209}Bi nuclide are generally in good agreement with the ENDF/B-VI data.

Reference

1) Y.Uno, Y.Uwamino, T.S.Soewarsono and T.Nakamura, Nucl. Sci. Eng. 122, 247 (1996).
2) N.Nakao, H.Nakashima, T.Nakamura, Sh. Tanaka, S.Tanaka, K.Shin, M.Baba, Y.Sakamoto and Y.Nakane, Nucl. Sci. Eng. 124, 228 (1996).
3) T.Nakamura, Proceeding of the 30th Midyear Topical Meeting, San Jose, California, 1997, published by Health Physics Society, p.143
4) K.Komura, INS-TCH-9, Institute for Nuclear Study, University of Tokyo(1974)
5) T.Nakamaura and T.Suzuki, Nucl, Instrum. Methods, 205 211(1983)
6) W.R.Nelson, H.Hirayama and D.W.O.Rogers, The EGS4 Code System, SLAC-265, Stanford Linear Accelerator Center, Stanford University (1985)
7) A.Torii, Y.Uwamino and T.Nakamura, INS-T-468, Institute for Nuclear Study, University of Tokyo(1987)
8) National Nuclear Data Center, Brookhaven National Laboratory, ENDF/B-VI(1990)
9) V.MaLane, C.L.Dunford and P.F.Rose, Vol.2, Neutron Cross Section Curves, Academic press., New York (1988)
10) O.dano and S. Iwasaki, Proceeding s of 1993 Symposium on Nuclear Data, Tokai, Japan, 1994, Edited M. Kawai and T. Tokio, p.310
11) M.Blann, CODE ALICE/89, Private communication (1989)

Table I. Physical data of irradiation samples

Facility	Sample	Diameter	Thickness	Weight	Purity
INS	^{12}C	20mm	2.2mm	1.57g	98.81%
	^{27}Al	30mm	2.0mm	3.80g	99.99%
	^{209}Bi	15mm	0.6mm	0.65g	99.99%
TIARA	^{12}C	33mm	1.0mm	1.83g	98.81%
	^{27}Al	33mm	1.0mm	3.00g	99.99%
	^{59}Co	33mm	2.0mm	20.0g	99.99%
	^{nat}Cu	33mm	2.0mm	20.0g	99.99%
	^{209}Bi	80mm	2.0mm	6.90g	99.99%
RIKEN	^{12}C	80mm	10.0mm	104g	98.81%
	^{27}Al	80mm	10.0mm	140g	99.99%
	^{nat}Cu	80mm	10.0mm	490g	99.99%
	^{209}Bi	80mm	10.8mm	530g	99.99%

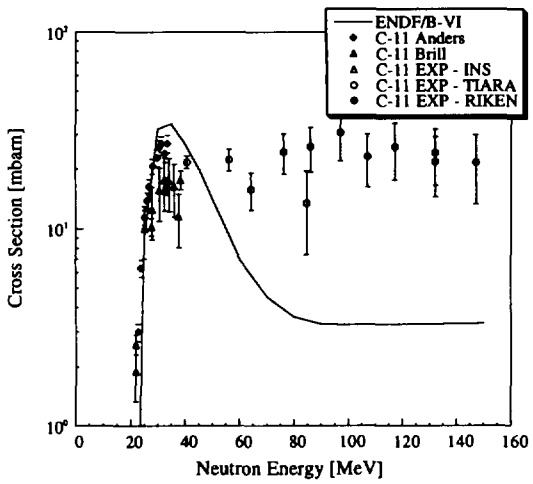

Fig.1 $^{12}C(n,2n)^{11}C$ Reaction Cross Section

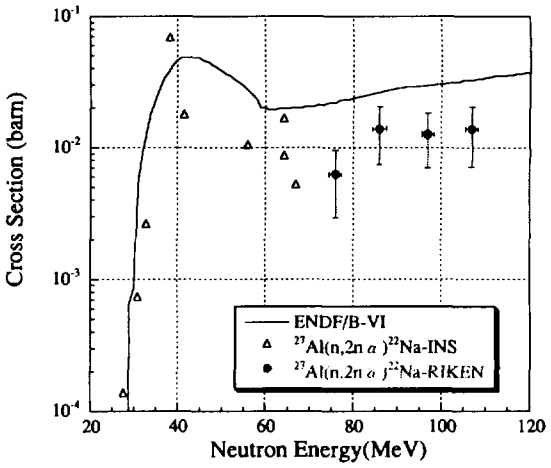

Fig.2 $^{27}Al(n,2n\alpha)^{22}Na$ Reaction Cross Section

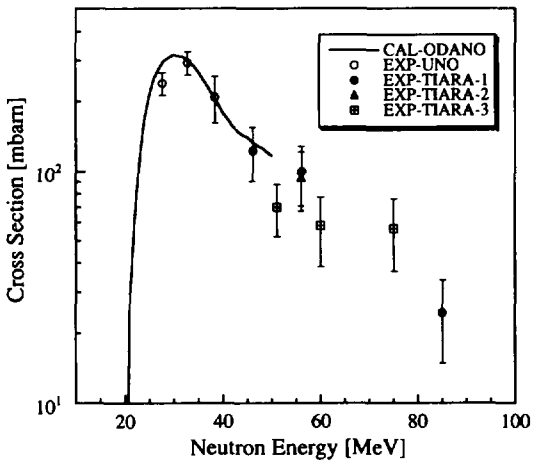

Fig. 3 $^{59}Co(n,3n)^{57}Co$ Reaction Cross Section

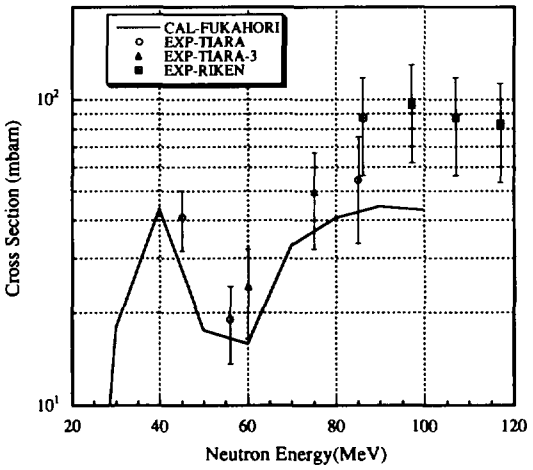

Fig.4 $^{nat}Cu(n, sp)^{58}Co$ Reaction Cross Section

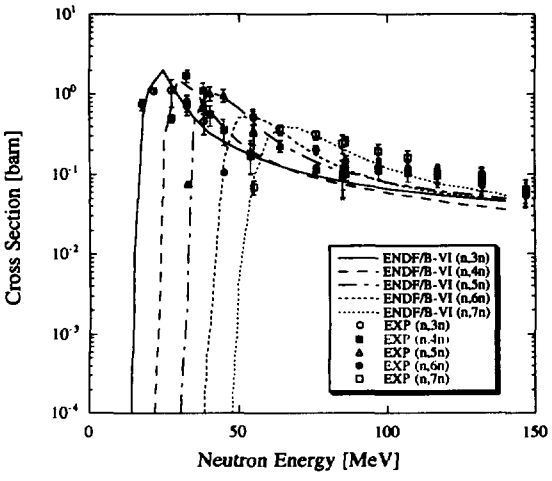

Fig.5 $^{209}Bi(n,xn)$ (x=3, 7) Reaction Cross Section

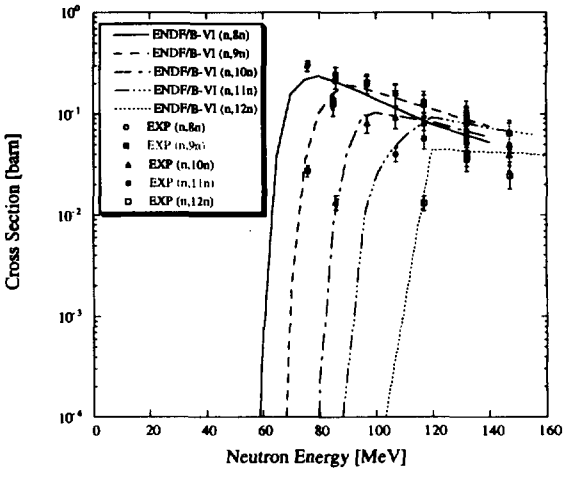

Fig. 6 $^{209}Bi(n,xn)$ (x=8,12) Reaction Cross Section

VIII-C-2

Measurements of secondary neutrons produced from thick targets bombarded by heavy ions

T.Kurosawa[1], T.Nakamura[1], N.Nakao[2], T.Shibata[2]
Y.Uwamino[3], N.Nakanishi[3], A.Fukumura[4], Y.Kumamoto[4]

1. Introduction

At the National Institute of Radiological Sciences, the HIMAC accelerator (Heavy Ion Medical Accelerator in Chiba) is routinely used for the heavy ion cancer therapy. During operation of this machine, we started to measure the angular and energy distributions of secondary neutrons, from thick targets bombarded by helium, carbon and neon ions, whose experimental data are very scarce. These data are needed to design shielding for the heavy-ion accelerator facility, and also are of interest for estimating neutron doses producted by nuclear interactions during irradiation of tumors with heavy ions.

2. Experimental Procedure

The target materials with the thicknesses and the incident energies of carbon, helium and neon ions are shown in Table 1. All targets have a shape of 10cm by 10cm square. The target thickness was determined to stop the incident particles completely. Fig. 1 shows the experimental arrangement at HIMAC. We used three sets of NE213 organic liquid scintillator (12.7cm diam. by 12.7cm-long) for E counter and NE102A plastic scintillator (15cm by 15cm and 0.5cm thickness) for ΔE counter. A thin NE102A plastic scintillator (3cm diam. by 0.05cm thickness) was set for beam pick-up near by the end of the beam line, and the output pulses of this scintillator were used as start signals of the TOF measurement and also to count the absolute number of beam particles incident on the target. For discriminating between neutrons and charged particles, we used the output pulses of the ΔE counter that was placed just in front of each E counter, and charged particles were identified from two-dimensional ΔE-E graphical plots.

The contribution of the background neutrons caused by the room-scattering was measured at 90 degree placing a rectangular iron block with the size of 15cm by 15cm by 60cm long between the target and the detector.

The beam pick-up timing signal started a 2048 channel CAMAC time-to-digital converter (TDC). Anode signals of the photomultipliers, which were connected to the NE213 scintillators, were divided into three pulses. One pulse was put into CFD to produce the start signal of TDC.Two pulses were put into ADCs that collected the charge of pulse during the gate signal duration. In order to reject the events induced by gamma rays, the two-gate integration method[1] , total gate and slow gate, was adopted. The total gate also employed to measure the pulse height of the scintillation.

[1]*Cyclotron and Radioisotope Center , Tohoku University*
[2] *High Energy Accelerator Research Organization*
[3]*The Insutitute of Physical and Chemical Research*
[4]*National Institute of Radiological Sciences*

3. Data Analysis

For discrimination between neutrons and charged particles, we used the output pulses of the ΔE couter, and charged particles were identified from two-dimensional ΔE-E graphical plots. After the neutron and gamma ray (neutral charge) events were distinguished from the charged particle events, the neutron events and the gamma ray ones were separated using two dimensional total-slow pulse height graphical plots. Thus the TOF spectrum of neutrons was obtained and was converted into the energy spectrum of neutrons by the following expression,

$$\Phi(E) = \frac{C(E, L_{th})}{\varepsilon(E, L_{th}) \cdot \Delta E \cdot Q \cdot \Delta\Omega} \cdot f_d$$

where $C(E, L_{th})$ is the energy distribution of neutron counts, ΔE the energy bin, $\Delta\Omega$ the solid angle sustained by the detector to the center of the target, Q the incident heavy ion counts, f_d the correction of dead time, $\varepsilon(E, L_{th})$ the detection efficiency for neutron, L_{th} the discrimination level for the neutron pulse height, $\Phi(E)$ the neutron energy spectrum. The detection efficiencies were calculated with the Cecil code[2].

4.Results

4.1. Neutron spectra

As an example, secondary neutron spectra from carbon and lead targets for 400MeV/nucleon carbon incidence are shown in Figs.2 and 3. These spectra in the forward direction have a broad peak at high energy end, especially a large bump at 0 degree and this peak becomes more prominent for lighter target and for higher projectile energy. The peak energy of this bump is about 60 to 70% of the projectile energy per nucleon. This means that these high energy neutron components produced in the forward direction by knock-on collision and the momentum transfer from projectile to target nuclei are both higher for lighter nucleus and higher projectile energy than for heavier nucleus and lower projectile energy.

The neutron spectra have two components: One below about 10MeV corresponds to neutrons produced isotropically in the center of mass system mainly by the equilibrium process; the other above 10MeV corresponds to those produced by the preequilibrium process. Since the neutron emission by the preequilibrium process has a sharp forward peaking of the angular distribution, the neutron spectra become softer at larger emission angles, where the equilibrium process is prominent.

The high energy neutrons in the forward direction spread up to about the energy which is equivalent to the twice of the incident particle energy per nucleon.

4.2. Angle distribution

The neutron yields integrated above 5MeV are shown in Fig. 4-7. All of the results suggest that the neutron yield is larger for lighter target nucleus in the forward direction while at large angles the yield is larger for heavier target nucleus. This means that the neutron production at the forward angle mainly occurs by the direct reaction process which reduces in magnitude with increase of emission angle, and at the large angle the low energy neutrons via equilibrium process dominate. The former production process gives that the momentum transfer from a heavier projectile to a lighter target is

greater and the velocity of the center of mass is greater in the laboratory system; then based on the kinematics, a nucleon is emitted in the more forward direction from the heavier projectile and the lighter target. The latter process is proportional to the nucleon numbers that the heavier target have higher values than the lighter target.

5.Conclusins

We measured neutron angular and energy distributions produced by helium, carbon and neon ions stopping in targets of carbon, aluminum, copper, and lead. We are also proceeding the experiments for other heavy ions with several energies.

References

1) Z.W.Bell, Nucl. Instrum. Meth., 188, 105(1981).

2) R.A.Cecil, et al., Nucl. Instrum. Meth., 161, 439(1979).

Table 1 Projectile and target combinations and detector positions for measuring the secondary particles.

Incident particle energy[MeV]	Target thickness [cm]	Detector position [degree]
C [100]	C [2] Al [2] Cu [0.5] Pb [0.5]	0, 7.5, 15, 30, 60, 90
C [180]	C [6] Al [4] Cu [1.5] Pb [1.5]	0, 7.5, 15, 30, 60, 90
C [400]	C [20] Al [15] Cu [5] Pb [5]	0, 7.5, 15, 30, 60, 90
He [100]	C [5] Al [4] Cu [1.5] Pb [1.5]	0, 7.5, 15
He [180]	C [16] Al [12] Cu [4.5] Pb [5]	0, 7.5, 15, 30, 60, 90
Ne [400]	C [11] Al [9] Cu [3] Pb [3]	0, 7.5, 15, 30, 60, 90

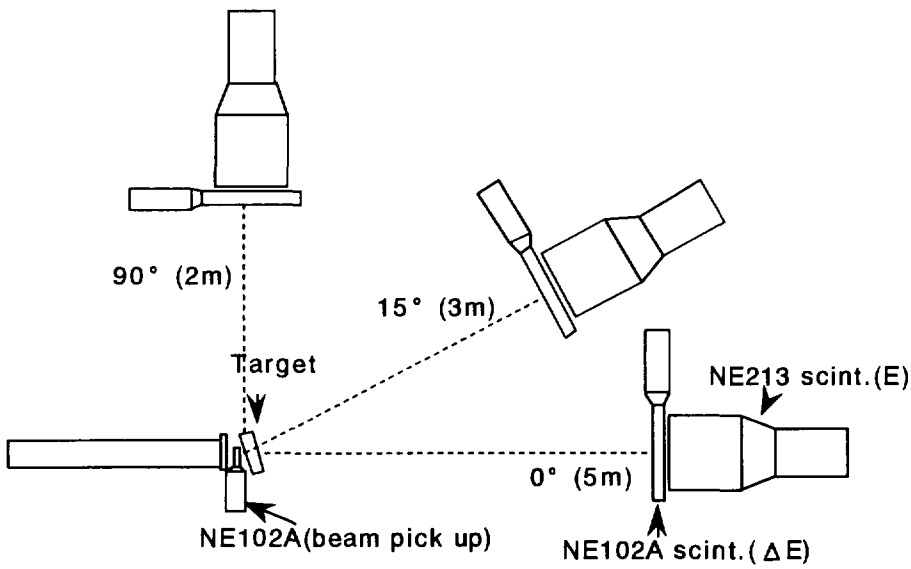

Fig. 1 Experimental arrangement at HIMAC

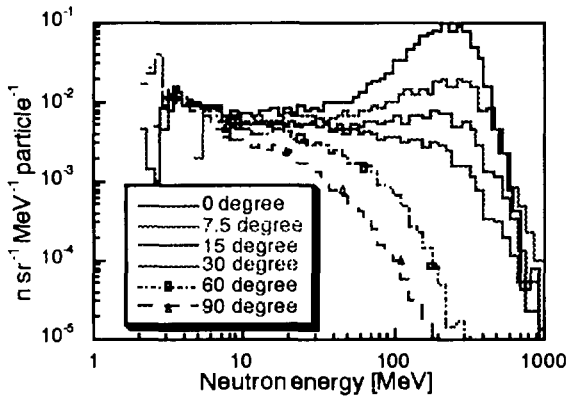

Fig. 2 Neutron spectra from 400MeV/u carbon ions in carbon target.

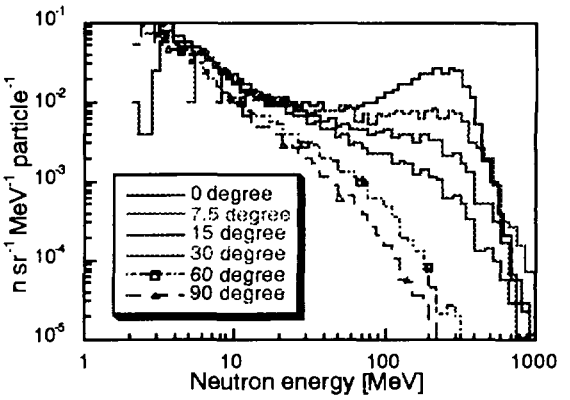

Fig. 3 Neutron spectra from 400MeV/u carbon ions in lead target.

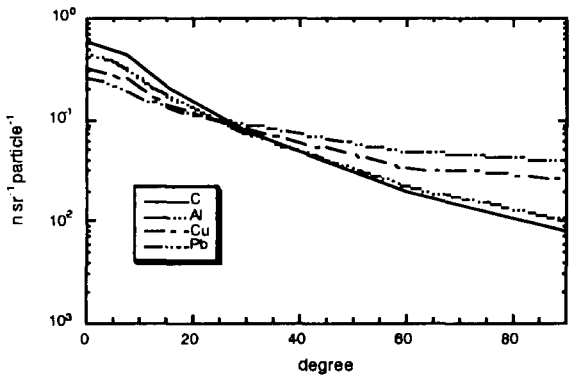

Fig. 4 Neutron yields integrated above 5MeV from 100MeV/u helium ions.

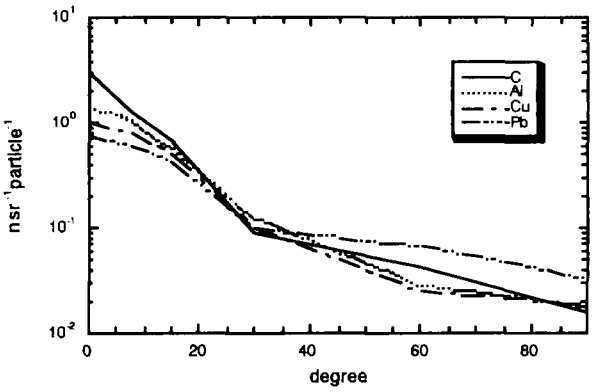

Fig. 5 Neutron yields integrated above 5MeV from 180MeV/u helium ions.

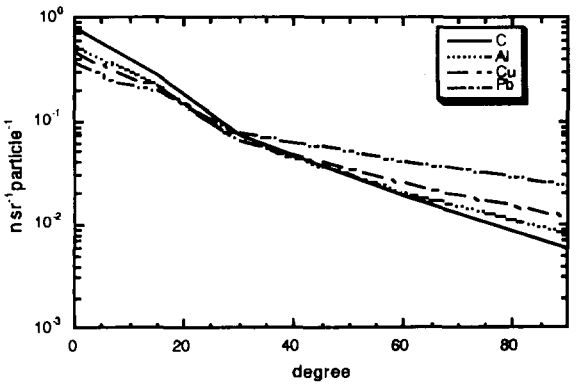

Fig. 6 Neutron yields integrated above 5MeV from 100MeV/u carbon ions.

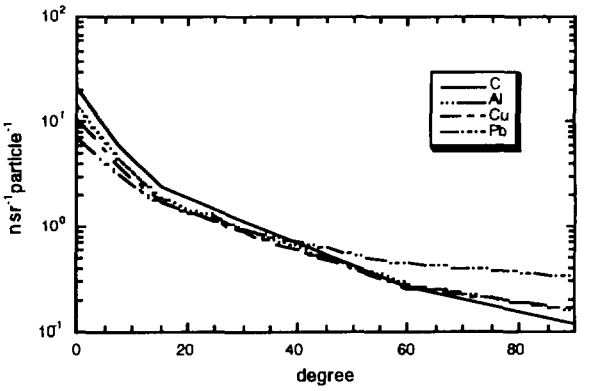

Fig. 7 Neutron yields integrated above 5MeV from 400MeV/u carbon ions.

IX. Tokyo Institute of Technology

IX-1 Low-energy neutron direct capture by ^{12}C in a dispersive optical potential

H. Kitazawa, K. Go, and M. Igashira

A paper of this subject was published in Phys. Rev. C57, 202(1998), with the following abstract.

A dispersive optical potential for the interaction between low-energy neutrons and ^{12}C-nuclei is derived from a dispersion relation based on the Feshbach generalized optical model. The potential reproduces completely neutron total cross sections below 1.0 MeV, and substantially the energy of the 3090 keV($1/2^+$) level in ^{13}C which is of nearly-pure $2s_{1/2}$ single-particle character. It is found that direct-capture model calculations with this potential explain quite successfully observed off-resonance capture transitions to the ground($1/2^-$), 3090 keV($1/2^+$), 3685 keV($3/2^-$), and 3854 keV($5/2^+$) levels in ^{13}C at neutron energies of 20-600 keV. Special emphasis is laid on the fact that in those model analyses, account should be taken of the spatial nonlocality of the neutron-nucleus interaction potential, in particular for negative energies.

IX-2 Measurement of $^1H(n, \gamma)^2H$ reaction cross section at a comparable $M1/E1$ strength

Y. Nagai, T. S. Suzuki, T. Kikuchi, T. Shima, T. Kii, H. Sato, and M. Igashira

A paper of this subject was published in Phys. Rev. C56, 3173(1997), with the following abstract.

The cross section of the $p(n, \gamma)d$ reaction was directly measured for the first time at E_n=550 keV, where the theoretical $E1$ transition strength is comparable to the $M1$ strength. It was determined accurately to be 35.2(24) μ b, and it agrees with the theoretical one which includes the meson-exchange currents. In this work, a prompt discrete γ-ray detection method combined with a pulsed neutron beam and a newly developed Monte Carlo code was essential to obtain an accurate cross section.

IX-3 Measurements of keV-Neutron Capture γ Rays of Fission Products and Structural Materials

M. Igashira, S. Mizuno, T. Ohsaki, and H. Kitazawa

γ rays from the keV-neutron capture reactions by ^{51}V,^{55}Mn,^{140}Ce,^{141}Pr,$^{147,150,152,154}Sm$, ^{153}Eu,and ^{162}Dy have been measured at a neutron energy of 550 keV, using a large anti-Compton NaI(Tl) γ-ray spectrometer and the $^{7}Li(p,n)^{7}Be$ pulsed neutron source with a 3-MV Pelletron accelerator. The preliminary results for the capture cross sections and γ-ray spectra of those nuclei are obtained.[1)]

Reference:

1) M. Igashira et al.: Proc.Int.Conf.on Future Nuclear Systems, Yokohama, Japan, October 5-10, 1997, p.1360(1997)

IX-4 Low-Energy Neutron Direct Capture by ^{16}O

H. Kitazawa and M. Igashira

A paper of this subject was presented at the 1997 Symposium on Nuclear Data, Tokai, Japan, November 27-28, 1997, with the following abstract.

Low-energy neutron capture reactions on light nuclei play an important role in the nucleosynthesis on the inhomogeneous big-bang model as well as in the s-process nucleosynthesis in red giant stars. Furthermore, drip-line light nuclei are found to have radii much larger than those of other neighboring nuclei[1]. This suggests the existence of a neutron-halo stucture in the nuclei.

Stimulated by the above findings, a lot of experimental work has recently been performed to obtain off-resonance neutron-capture cross sections of light nuclei in the steller energy region[2-4]. Simultaneously, these cross sections have been evaluated by Mengoni *et al.*[5], Otsuka *et al.*[6], and Kitazawa *et al.*[7] in the framework of a direct-capture model, because the reactions may be decoupled from resonance excitation. In particular, Kitazawa *et al* have used a dispersive optical model to achieve consistency between capture and scattering. In the present study, a dispersive optical potential for the interaction between

low-energy neutrons and ^{16}O-nuclei is derived from a dispersion relation based on the Feshbach generalized optical model, following our previous work[7]. This potential is applied to direct-capture model calculations in explaining off-resonance neutron-capture cross sections of ^{16}O observed at 20-70 keV[8]. The model calculations take account of the spatial nonlocality of the neutron-nucleus interaction potential.

References

[1] I. Tanihata, H. Hamagaki, O. Hashimoto, Y. Shida, N. Yoshikawa, K. Sugimoto, O. Yamakawa, and T. Kobayashi : Phys. Rev. Lett., 55, 2676(1985).

[2] Y. Nagai, M. Igashira, K. Takeda, N. Mukai, S. Motoyama, F. Uesawa, H. Kitazawa, and T. Fukuda : Astrophys. J., 372, 683(1991).

[3] T. Ohsaki, Y. Nagai, M. Igashira, T. Shima, K. Takeda, S. Seino, and T. Irie: Astrophys. J., 422, 912(1994).

[4] M. Igashira, Y. Nagai, K. Masuda, T. Ohsaki, and H. Kitazawa : Astrophys. J., 441, L89(1995).

[5] A. Mengoni, T. Otsuka, and M. Ishihara : Phys. Rev., C52, R2334(1995).

[6] T. Otsuka, M. Ishihara, N. Fukunishi, T.Nakamura, and M. Yokoyama : Phys. Rev., C49, R2289(1994).

[7] H. Kitazawa, K. Go, and M. Igashira : Proc. 9th Int. Symp. On Capture Gamma-ray Spectroscopy and Related Topics, Budapest, Hungary, October 8-12, 1996; to be published in Phys. Rev. C.

[8] M. Igashira : private communication.

IX-5 Measurements of Gamma Rays from keV-Neutron Resonance Capture by Odd-Z Nuclei in the 2s-1d Shell Region

M. Igashira, S. Y. Lee, S. Mizuno, J. Hori, and H. Kitazawa

A paper of this subject was presented at the 1997 Symposium on Nuclear Data, Tokai, Japan, November 27-28, 1997, with the following abstract.

For the last decade, we measured capture gamma rays from broad keV-neutron resonances of 1p shell and 2s-1d shell nuclei to study resonance capture mechanisms[1], using an anti-Compton NaI(Tl) gamma-ray spectrometer because the detection efficiency of NaI(Tl) was much larger than that of Ge(Li) or HPGe detector. For odd-Z nuclei, however,

the energy resolution of NaI(Tl) is not enough because the level spacing of residual nucleus is so small that some gamma rays cannot be resolved.

On one hand, large HPGe detectors are available at present, and it becomes possible to apply a large HPGe detector to our resonance experiment. Therefore, we have constructed an anti-Compton HPGe spectrometer with 100% relative efficiency[2], and started systematic measurements of keV-neutron resonance capture gamma rays for odd-Z nuclei in the 2s-1d shell region, using pulsed keV-neutrons produced from the $^{7}Li(p,n)^{7}Be$ reaction by bombarding a Li-evaporated copper disk with a 1.5-ns bunched proton beam from the 3-MV Pelletron accelerator of the Research Laboratory for Nuclear Reactors at the Tokyo Institute of Technology.

A series of measurements for ^{19}F, ^{23}Na and ^{27}Al has been performed, and capture gamma rays from the 27-, 49-, and 97-keV resonances of ^{19}F, the 35- and 53-keV resonances of ^{23}Na, and the 35-keV resonance of ^{27}Al were observed. Some results are presented in this contribution.

References

[1] H. Kitazawa and M. Igashira, Proc. Specialists' Meeting on Measurement, Calculation and Evaluation of Photon Production Data, NEA/NSC/DOC(95)1 (1995) 169.

[2] M. Igashira et al., Proc. the 8th Int. Symp. on Capture Gamma-Ray Spectroscopy and Related Topics, 1993, p.992.